Available online at www.ijournalse.org

Emerging Science Journal

(ISSN: 2610-9182)

Vol. 10, No. 2, April, 2026

Mg, Si, Al, and P Particle-Doped Epoxy: A Synergistic Approach for Enhanced Fire Performance

Qandeel Fatima Gillani [1], Almagul Mentbayeva [1*], Muhammad Faisal Javed [2], Sandugash Kalybekkyzy [3]

[1] *School of Engineering and Digital Sciences, School of Engineering and Digital Sciences, Nazarbayev University, Astana 010000, Kazakhstan.*

[2] *Department of Civil Engineering, GIK Institute of Engineering Sciences and Technology, Topi, Swabi 23460, Pakistan.*

[3] *School of Sciences and Humanities, Nazarbayev University, Nur-Sultan 010000, Kazakhstan.*

Abstract

This study presents the development of a low-toxicity, high-performance intumescent fire-retardant coating (IFRC) through a hybrid epoxy binder doped with Mg, Si, Al, and P particles. The objective was to improve thermal stability and char cohesion and reduce the toxic aromatic emissions typically released from bisphenol-A epoxy systems during combustion. Modified epoxy resins were prepared by dispersing $Mg(OH)_2$ and incorporating hydroxyl-terminated PDMS, followed by formulation with APP, melamine, expandable graphite, PER, and nano-alumina. Comprehensive analyses using FTIR, ^{13}C NMR, DSC, TGA, SEM–EDS, TEM, XRD, and GC–MS, along with ISO-834 furnace and ASTM E-119 flame tests, were employed to evaluate chemical structure, thermal behavior, char morphology, and fire performance. The optimized formulation produced a dense Mg–Al–silicate–phosphate char network, achieved a 6.1× expansion ratio, limited backside steel temperature to 227°C, and retained 36% char at 800°C, which significantly outperformed the unmodified epoxy system. GC–MS confirmed a substantial (≈53%) reduction in toxic volatile emissions. A machine-learning model further validated char compactness with >94% classification accuracy. Collectively, the results demonstrate that synergistic inorganic–siloxane modification offers a scalable, halogen-free pathway to next-generation epoxy-based IFRCs with enhanced fire resistance and markedly lower toxicity.

Keywords:

Char Morphology;
Condensed-Phase Mechanism;
Fire Protection Coatings;
Siloxane Modification;
Thermal Degradation;
Toxic Emission Reduction.

Article History:

Received:	11	November	2025
Revised:	08	March	2026
Accepted:	16	March	2026
Published:	01	April	2026

1- Introduction

Epoxy resins are widely used in industrial, construction, and transportation sectors due to their excellent mechanical strength, adhesion, and chemical resistance; however, their high flammability and release of toxic smoke during combustion present serious limitations for fire-critical applications [1-4]. Conventional intumescent fire-retardant coatings (IFRCs) based on acid, carbon, and gas-forming systems—including ammonium polyphosphate (APP), pentaerythritol (PER), melamine (MEL), and expandable graphite (EG)—offer an effective halogen-free strategy by generating a protective char barrier, yet they still face issues such as poor adhesion to epoxy matrices, limited stability of the swollen layer, and incomplete suppression of toxic gas emissions [5-7]. To enhance the thermal resistance of epoxy systems, researchers have explored reactive phosphorus-nitrogen compounds [8-10], ceramic-forming fillers [11-13], microencapsulated APP [14], layered double hydroxides (LDHs) [13, 15-17], halloysite nanostructures [18-21], and natural carbon sources like lignin and nanocellulose [22-26].

* **CONTACT**: almagul.mentbayeva@nu.edu.kz

DOI: https://doi.org/10.28991/ESJ-2026-010-02-021

Although these approaches improve thermal protection to varying degrees, most remain constrained by phase incompatibility with epoxy, high viscosity during processing, limited char cohesion under prolonged heat flux, and insufficient reduction of toxic volatiles such as aromatics, carbonyls, and phosphoric species [27-30]. In particular, studies incorporating metallic hydroxides (Mg/Al) [31, 32], siloxane-based modifiers [33-35], and phosphorus-containing compounds [36-38] highlight promising fire performance enhancements, but they typically evaluate these additives independently rather than as part of a unified binder-engineering strategy. As a result, the fundamental chemical interaction between inorganic fillers and siloxane domains within an epoxy matrix and its influence on char chemistry, crosslinking, and gas-phase suppression remains poorly understood [38-40].

Recent work has indicated that magnesium hydroxide ($Mg(OH)_2$) can promote char stability by releasing MgO, which acts as a ceramic catalyst and reinforces the protective layer during combustion [41]. Parallel efforts on siloxane-modified epoxy networks demonstrate improved thermal stability, flexibility, and formation of Si–O–Si/Si–C ceramic residues [13, 42, 43]. However, existing literature has not investigated their combined effect in a single pre-engineered binder system, particularly in the presence of conventional IFRC additives (APP, MEL, PER, EG). Moreover, most studies overlook the synergistic condensed-phase mechanism that may occur when MgO interacts with siloxane domains, enabling the formation of hybrid Mg–O–Si char architectures, which can significantly enhance the barrier's mechanical integrity and reduce the evolution of toxic decomposition products [44]. Another key gap is the limited mechanistic analysis of volatile organic compounds generated during epoxy breakdown; only a few studies have employed pyrolysis-GC/MS to quantify aromatic and carbonyl emissions in modified IFRC systems [45-47]. Additionally, despite growing interest in predictive data-driven modeling, machine-learning-assisted char analysis has rarely been applied to evaluate modified epoxy IFRCs. These deficiencies indicate that there must be a comprehensive study integrating chemical binder modification, condensed-phase mechanistic validation, and emission-profile analysis.

To address these gaps, the present work develops a novel $Mg(OH)_2$-dispersed and siloxane-integrated epoxy binder engineered specifically for intumescent systems. Unlike previous studies that rely on physically blended additives, we chemically introduce hydroxyl-terminated siloxane into $Mg(OH)_2$-dispersed bisphenol-A epoxy, enabling in-situ formation of Mg–O–Si linkages and improved compatibility with IFRC components. This dual-functional binder is hypothesized to enhance char expansion, promote ceramic-like residue formation, and significantly suppress toxic volatiles during combustion. The theoretical basis of our approach lies in the synergistic condensed-phase mechanism: $Mg(OH)_2$ thermally decomposes to MgO, which catalyzes crosslinking and strengthens the siloxane-rich char, while siloxane domains contribute flexible, thermally stable Si–O–Si structures capable of forming a cohesive protective layer. Through systematic characterization—including FTIR, XRD, SEM, TEM, TGA, DSC, and pyrolysis-GC/MS—we offer mechanistic knowledge about char chemistry and toxic gas suppression, complemented by machine-learning-assisted quantitative analysis.

The remainder of this article is organized as follows: Section 2 describes the synthesis of the modified epoxy binder and preparation of IFRC formulations; Section 3 presents the experimental characterization and testing procedures; Section 4 discusses the results related to thermal stability, char morphology, emission suppression, and fire performance; and Section 5 concludes with key findings and potential implications for next-generation epoxy-based intumescent coatings.

2- Materials and Methods

2-1- Materials

Bisphenol-A epoxy resin (DGEBA type), poly(dimethylsiloxane) (PDMS, hydroxyl-terminated), magnesium hydroxide ($Mg(OH)_2$, ≥99%), ammonium polyphosphate (APP), melamine (MEL), expandable graphite (EG), and pentaerythritol (PER) were used as received. All reagents were of analytical grade and sourced from commercial suppliers. A polyamide-based curing agent was employed for crosslinking the epoxy system. Solvents used for dispersion and washing were of analytical grade purity.

2-2- Preparation of PDMS-Modified $Mg(OH)_2$-Doped Epoxy Resins

A series of epoxy–PDMS hybrid resins (denoted as MER-0 to MER-5) were synthesized via a two-step modification route. Initially, 2 wt% $Mg(OH)_2$ nanoparticles were dispersed into preheated bisphenol-A epoxy resin using a mechanical stirrer at 60 °C for 1 h, followed by ultrasonic agitation for 30 min to ensure homogeneous dispersion. Subsequently, hydroxyl-terminated PDMS was incorporated in varying proportions (0–50 wt%) relative to the epoxy matrix. Phosphoric acid (1 wt%) was introduced as a catalyst to promote the condensation and partial grafting between epoxy and PDMS chains through Si–O–C linkage formation. The resulting mixtures were stirred for 2 h at 70 °C until uniformity was achieved. The hybrid resins were designated as MER-0 (0% PDMS), MER-1 (10%), MER-2 (20%), MER-3 (30%), MER-4 (40%), and MER-5 (50%), as shown in Table 1. The formulation design was developed based on insights and strategies reported in previous studies [18, 19, 35, 39, 45, 47, 48].

Table 1. Formulation Details of Modified Epoxy Resin with varying PDMS Content

Formulation Name	Composition
MER-0	$Mg(OH)_2$-dispersed Bisphenol A epoxy resin.
MER-1	90% $Mg(OH)_2$-dispersed Bisphenol A epoxy resin + 10% PDMS.
MER-2	80% $Mg(OH)_2$-dispersed Bisphenol A epoxy resin + 20% PDMS.
MER-3	70% $Mg(OH)_2$-dispersed Bisphenol A epoxy resin + 30% PDMS.
MER-4	60% $Mg(OH)_2$-dispersed Bisphenol A epoxy resin + 40% PDMS.
MER-5	50% $Mg(OH)_2$-dispersed Bisphenol A epoxy resin + 50% PDMS.

2-3- Formulation of Intumescent Fire-Retardant Coatings (IFRCs)

Each modified resin (MER-0–MER-5) was used as a binder for the intumescent coating formulations, labeled IF-0–IF-5, respectively. The base composition of each formulation consisted of APP (10 wt%), MEL (10 wt%), EG (4.3 wt%), PER (4.3 wt%), nano-alumina (0.3 wt%), and epoxy resin with hardener (68 wt%), as shown in Table 2. The ingredients were mixed sequentially using a mechanical stirrer at 40 rpm for 1 h, followed by degassing under vacuum. The coatings were applied on mild steel panels (100 × 100 × 3 mm) using a bar coater to achieve a uniform dry film thickness of 1.5 ± 0.1 mm. Curing was performed at ambient conditions for 24 h, followed by post-curing at 80°C for 2 h, as shown in Figure 1.

3- Characterization Techniques

This section summarizes the analytical techniques used to evaluate the PDMS-modified $Mg(OH)_2$–epoxy resins and their corresponding intumescent fire-retardant coatings (IFRCs). Characterization was performed in two stages: Section 3.1 confirms the chemical structure and modification of the epoxy resins, while Section 3.2 assesses the thermal stability, morphological characteristics, and fire-protective performance of the developed IFRC systems.

Table 2. Composition of IFRCs with $Mg(OH)_2$ and PDMS-Modified Epoxy

Formulations	(APP)	(MEL)	(BA)	(PER)	(EG)	Nano Alumina	Epoxy resins (MER)	Hardener
	wt. %age (gm)	wt. %age (gm)	wt. %age (gm)	wt. %age (gm)	wt. %age (gm)	wt. %age (gm)	wt. %age (gm)	wt. %age (gm)
IF-0	10	4.5	10	2.5	4.3	0.3	45.7(MER-0)	22.7
IF-1	10	4.5	10	2.5	4.3	0.3	45.7(MER-1)	22.7
IF-2	10	4.5	10	2.5	4.3	0.3	45.7(MER-2)	22.7
IF-3	10	4.5	10	2.5	4.3	0.3	45.7(MER-3)	22.7
IF-4	10	4.5	10	2.5	4.3	0.3	45.7(MER-4)	22.7
IF-5	10	4.5	10	2.5	4.3	0.3	45.7(MER-5)	22.7

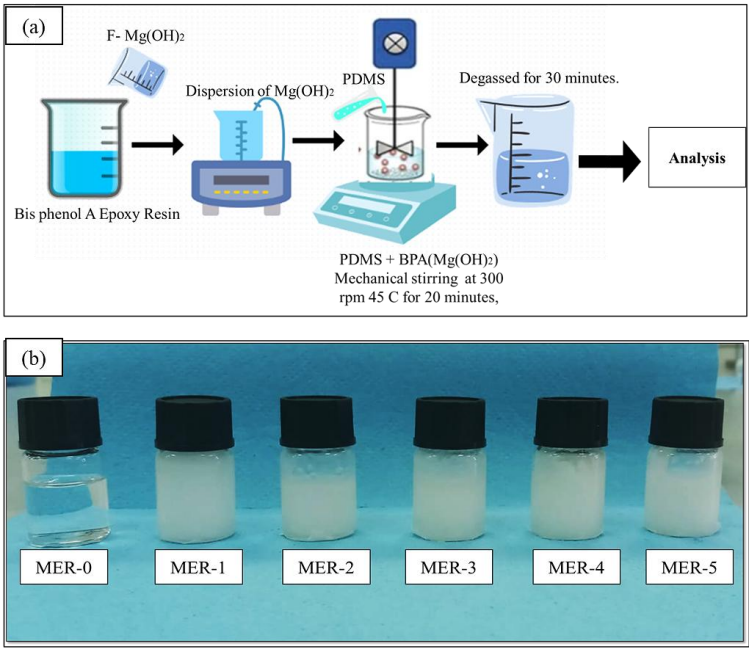

Figure 1. (a) Schematic illustration of the preparation process for Mg/Si doped epoxy resin. (b) Photograph of modified epoxy resin batches (MER-0 to MER-5) after synthesis, showing increasing turbidity and opacity with increasing PDMS content

3-1- Characterization of Modified Epoxy Resins

The viscosity of the modified epoxy resins was determined using an RH10 capillary rheometer at 25°C to assess the influence of PDMS incorporation on the rheological behavior of $Mg(OH)_2$-dispersed systems. Structural modifications and siloxane incorporation were confirmed through ATR-FTIR spectroscopy (Bruker Alpha II, 4000–400 cm^{-1}) and ^{13}C-NMR analysis (JEOL JNM-ECA 500, 500 MHz, $CDCl_3$ solvent), which provided insight into aromatic carbon reduction and Si–O linkage formation. The 13C NMR spectra were further normalized using a stable aliphatic epoxy backbone peak to allow distinction between dilution effects and structural modifications. Thermal stability and degradation characteristics were investigated using a Simultaneous Thermal Analyzer (STA 449 F5 Jupiter, NETZSCH) coupled with a Quadrupole Mass Spectrometer (QMS 403 Aeolos Quadro). Samples were heated from 50°C to 830°C under nitrogen at 10°C/min to determine decomposition temperatures, char yield, and evolved gas profiles.

3-2- Characterization of IFRCs Based on Modified Epoxy Resins

3-2-1- Fire Testing and Char Analysis

Fire performance was evaluated by furnace testing at 800°C for 60 min and ASTM E-119 Bunsen burner tests at 1350°C for 60 min using coated steel plates (10 × 10 cm). Backside temperature was continuously recorded with K-type thermocouples. Char expansion ratios and thickness were measured at multiple points to assess insulation effectiveness.

3-2-2- Microstructural and Elemental Characterization

The morphology and microstructure of the char residues were examined via Scanning Electron Microscopy (SEM, ZEISS Crossbeam 540), while Energy-Dispersive X-ray Spectroscopy (EDS) provided elemental composition and distribution data. Transmission Electron Microscopy (TEM, JEOL JEM–1400Plus) was used to observe nanoscale features and confirm siloxane dispersion within the char matrix.

3-2-3- Machine Learning-Based Quantitative Char Analysis

A supervised Convolutional Neural Network (CNN) framework was developed using TensorFlow/Keras to classify SEM images of char residues from all six formulations (IF-0–IF-5). Images were grouped into porous (P), intermediate (I), and dense (D) classes to correlate morphology with fire performance. A pre-trained EfficientNetB0 backbone with a custom classifier head achieved >94% accuracy in distinguishing structural classes. Interpretability was enhanced using Grad-CAM visualizations to identify morphology regions critical to model predictions. While the framework demonstrated strong performance, further expansion of the dataset and k-fold validation were recommended to improve generalizability.

3-2-4- Chemical and Structural Characterization

Post-combustion char residues were analyzed by FTIR spectroscopy (4000–400 cm^{-1}) to identify silicate and phosphate bonding features. Thermogravimetric analysis (TGA) was used to determine residual weight and char yield under identical conditions as Section 3.1.4. Pyrolysis–Gas Chromatography/Mass Spectrometry (Py–GC/MS, Thermo ITQ 700) was employed to identify volatile degradation products and assess emission toxicity reduction in modified coatings. X-ray Diffraction (XRD, Bruker D8 Quest, Cu Kα, $2\theta = 10°–80°$) determined the crystalline phases (silica, alumina, graphite, and metal phosphates) responsible for char stability.

The comprehensive characterization strategy integrated rheological, spectroscopic, thermal, and morphological analyses to elucidate structure–property relationships in the modified epoxy binders and their IFRCs. Advanced imaging combined with machine learning provided a quantitative link between char microstructure and fire performance, establishing a robust framework for the design of next-generation hybrid epoxy coatings.

4- Results and Discussion

4-1- Viscosity of Modified Epoxy Resins

The viscosity of each modified epoxy resin batch (MER-0 to MER-5) was measured to evaluate the flow characteristics of the binder system prior to its use in intumescent fire retardant coatings (IFRCs). Flowability is a critical factor in IFRC formulation, as it governs the ease of dispersion and homogeneous integration of intumescent additives such as ammonium polyphosphate (APP), melamine, expandable graphite (EG), and pentaerythritol (PER). $Mg(OH)_2$ was initially dispersed into bisphenol A epoxy resin and subsequently blended with varying proportions of hydroxyl-terminated polydimethylsiloxane (PDMS) to yield six resin formulations. As shown in Figure 2(a), a progressive increase in viscosity was observed with higher PDMS content. The rise in viscosity can be attributed to the interaction between hydroxyl-terminated PDMS and the epoxy resin matrix, which promotes physical entanglement and possibly chemical bonding between silanol (-SiOH) groups and epoxy functionalities. This phenomenon has been documented in siloxane-

modified epoxy systems, wherein the viscosity increment signifies the development of a partially cross-linked or extensively entangled network, even in the absence of curing agents [49]. Specifically, MER-5, which contains 50% PDMS, exhibited a viscosity exceeding 5000 cP. Such a high viscosity significantly limits its applicability as a binder for intumescent coatings. Highly viscous resin matrices tend to resist the proper dispersion of solid fillers, leading to poor homogeneity and processing difficulties at room temperature. Moreover, elevated viscosity reduces the free volume within the polymer matrix, impeding the uniform distribution of intumescent additives and nano-reinforcements such as nano-alumina. Such behavior often results in agglomeration of additives, diminished barrier performance, and inconsistencies in char expansion and thermal protection [50, 51].

In contrast, resin formulations with moderate PDMS content (MER-3 and MER-4) maintained a workable viscosity while still benefiting from the thermal stability and hydrophobic characteristics imparted by PDMS. These formulations allowed for uniform dispersion of all intumescent components and were easier to apply as coatings. The relationship between PDMS loading and viscosity must therefore be optimized to strike a balance between processability and performance [52]. Excessive PDMS content, while improving flexibility and thermal degradation characteristics, can adversely affect resin flow and additive compatibility—a key consideration in the formulation of functional IFRCs.

Recent studies on siloxane-epoxy hybrid systems report similar rheological trends, where increasing PDMS content leads to higher viscosity due to chain entanglement and reduced molecular mobility. For example, Chung et al. (2022) [53] showed that PDMS-grafted epoxy resins exhibit a sharp viscosity rise once siloxane exceeds 40 wt%, resulting in poor filler dispersion and phase separation. The behavior of MER-3 and MER-4 in the present study aligns closely with these findings, confirming the necessity of balancing siloxane loading to maintain processability while achieving enhanced thermal performance.

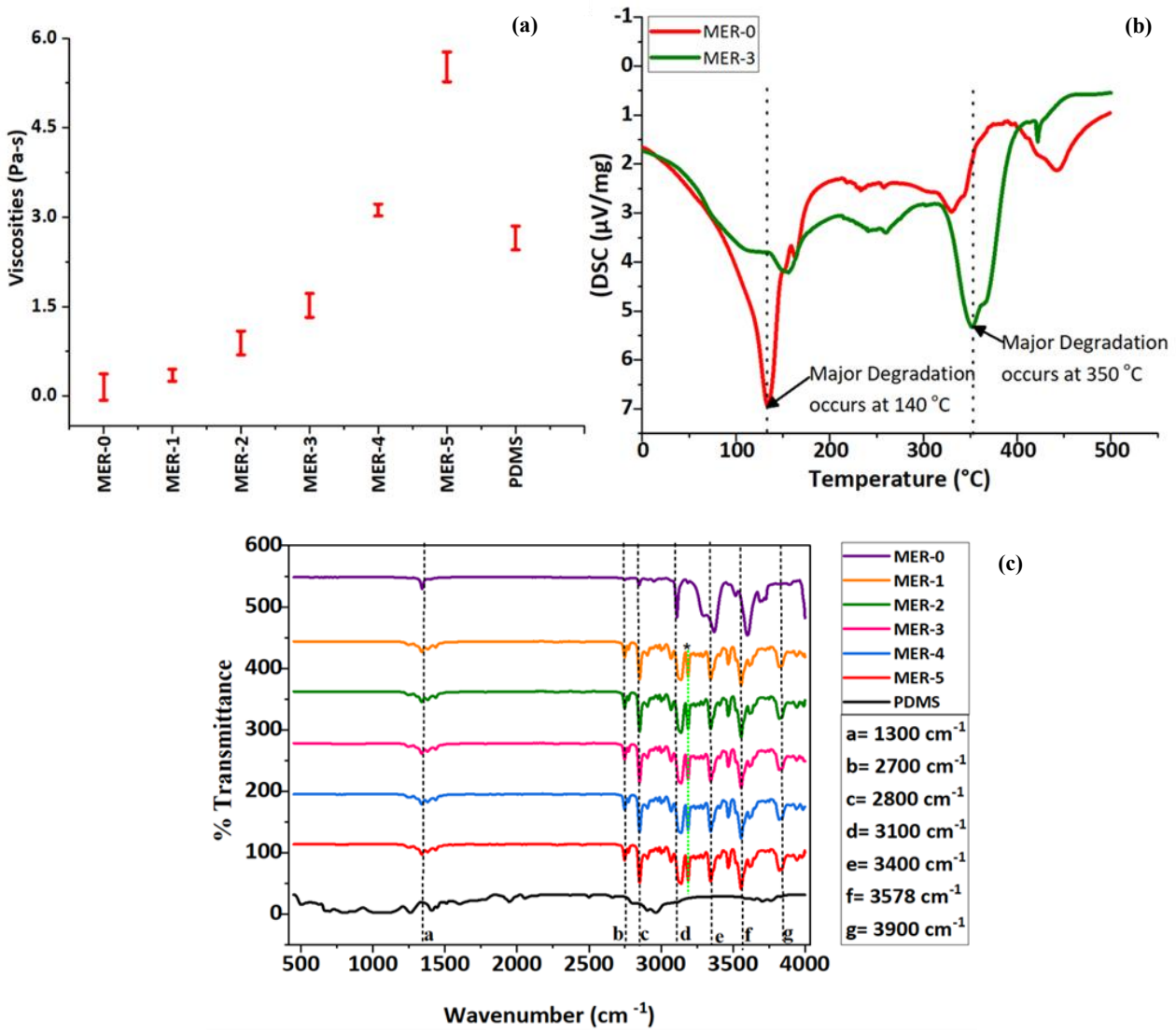

Figure 2. Comparative properties of modified epoxy resins: (a) viscosity (MER-0 to MER-5), (b) DSC thermo-grams of MER-0 versus MER-3 and (c) FTIR spectra of MER-0 to MER-5

4-2- FTIR Analysis of Modified Epoxy Resins

FTIR spectroscopy was carried out to confirm the successful incorporation and interaction of hydroxyl-terminated polydimethylsiloxane (PDMS) into the epoxy resin matrix. The structural evolution across the modified epoxy resin series (MER-0 to MER-5) provides clear evidence of both physical interactions and possible interfacial bonding between PDMS and the epoxy network. Figure 2(c) illustrates the transmittance spectra of the unmodified epoxy resin (MER-0), the pure PDMS, and the modified systems with increasing PDMS content. The spectrum of MER-0 exhibits characteristic epoxy bands, including C–O–C stretching near 1300 cm^{-1} (labelled "a"), and methylene/methyl asymmetric and symmetric C–H stretching vibrations around 2800–3100 cm^{-1} (bands "b" to "d") [54]. A broad –OH stretching band is evident near 3400 cm^{-1}, indicating the presence of free hydroxyl groups, either residual from the resin synthesis or resulting from interactions with surface hydroxyls of inorganic additives [55].

With the incremental addition of PDMS (MER-1 to MER-5), notable spectral shifts and intensity changes occur. Most importantly, new and stronger bands show up at 3200 cm^{-1} (marked with *), 3400 cm^{-1} ("e"), 3578 cm^{-1} ("f"), and 3900 cm^{-1} ("g"). These bands correspond to hydrogen-bonded and free hydroxyl stretching vibrations. The increasing prominence of these bands in higher PDMS-containing systems (especially MER-4 and MER-5) confirms the successful integration of PDMS chains, which contain terminal hydroxyl functionalities capable of interacting via hydrogen bonding with the epoxy matrix [56]. The observed broadening and red-shift of the O–H stretching bands in modified formulations further support the formation of strong intermolecular hydrogen bonds between siloxane and epoxy functional groups. The retention of characteristic epoxy peaks alongside PDMS-associated features suggests that the interaction is largely physical rather than covalent, as no new Si–O–C bond formation peaks (typically observed between 1000 and 1100 cm^{-1}) were detected [34]. This observation aligns with the uncured nature of the resin system, where hydroxyl–epoxy reactions have not yet been thermally initiated. In spectra of the modified epoxy resins, although, no distinct and isolated Si–O–C stretching band could be clearly resolved. This is attributed to the low concentration of newly formed Si–O–C linkages and their significant spectral overlap with dominant Si–O–Si vibrations from PDMS and C–O–C stretching of the epoxy network. Such overlap is well documented in siloxane-modified epoxy systems and limits the sensitivity of FTIR for unambiguous identification of Si–O–C bonds at early modification stages. Therefore, the absence of a clearly resolved Si–O–C band in FTIR does not imply the absence of chemical bonding.

Furthermore, as PDMS concentration increases, a gradual masking or attenuation of epoxy-related bands is evident. This spectral suppression is attributed to the dominant absorption of the PDMS matrix, which, owing to its flexible siloxane backbone, exhibits low IR transmittance in the fingerprint region [33]. The overall spectral evolution confirms that PDMS has been effectively incorporated into the epoxy matrix, forming a compatible hybrid phase. This structural compatibility is critical for tuning rheological and thermal properties in intumescent fire-retardant applications. The FTIR results strongly validate the successful physical integration of PDMS into the epoxy resin network via hydrogen bonding and phase entanglement. The changes in band intensities and positions are consistent with previously reported siloxane-epoxy systems [57], establishing MER-3 and MER-4 as optimal formulations for balancing compatibility, functionality, and processability in subsequent coating applications. Comparable spectral behavior has been reported in past literature on PDMS-modified epoxy matrices. Sobhani et al. (2012) [58] observed progressive intensification of O–H and Si–CH_3 bands with increased PDMS loading, consistent with hydrogen bonding and physical entanglement rather than extensive Si–O–C covalent formation. The FTIR trends observed in MER-1 to MER-5 show strong agreement with these earlier studies, validating the successful integration of PDMS within the epoxy backbone [59-61].

4-3- ^{13}C-NMR Analysis of Modified Epoxy Resins

To confirm the structural evolution of modified epoxy resins upon incorporation of hydroxyl-terminated polydimethylsiloxane (PDMS), solid-state ^{13}C NMR spectroscopy was conducted, presented in Figure A-2. The focus was on observing changes in the aromatic region (δ = 120–160 ppm) and aliphatic region (δ = 40–80 ppm), reflecting the transformation of bisphenol A epoxy (DGEBA)-based systems upon siloxane integration [62-64]. The control sample (MER-0) showed prominent aromatic peaks at 156.66, 143.66, 127.79, and 114.00 ppm, with a total signal intensity of 27.28 p.d.u., representing the characteristic aromatic backbone of BPA epoxy. Upon progressive addition of PDMS (MER-1 through MER-5), a significant decrease in aromatic signal strength was observed—down to 18.57, 9.21, 8.36, 8.35, and 10.42 p.d.u., respectively—indicating a 31.9% to 69.4% reduction compared to the unmodified resin.

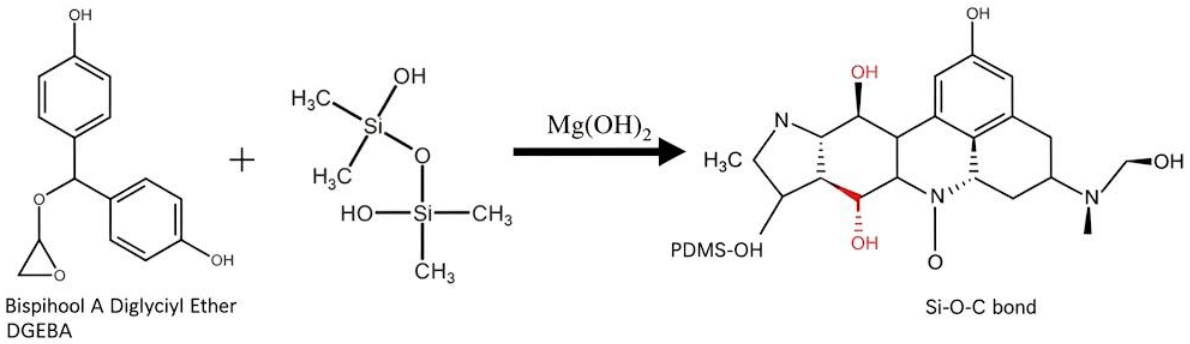

Figure 3. Illustrated pathway for the chemical modification of BPA epoxy resin through $Mg(OH)_2$-catalyzed condensation with hydroxyl-terminated PDMS

This reduction suggests that siloxane incorporation disrupts or masks the aromatic π-electron system. This behavior may arise from chemical interactions between hydroxyl-terminated PDMS and the epoxy or hydroxyl functionalities in the BPA backbone [65]. These interactions are facilitated by magnesium hydroxide [$Mg(OH)_2$], which plays a dual role—as a Lewis base catalyst promoting nucleophilic attack on the epoxy ring and as a dispersion aid improving compatibility between the organic matrix and inorganic filler [66]. The resulting mechanism involves $Mg(OH)_2$-catalyzed ring-opening of the strained oxirane ring in the BPA resin, forming a reactive alkoxide intermediate that undergoes condensation with PDMS terminal hydroxyl groups. This reaction leads to the formation of Si–O–C and Si–O–Mg linkages, effectively tethering PDMS chains to the epoxy backbone. As PDMS contains no aromatic rings and consists of flexible $–Si(CH_3)_2–O–$ units, its incorporation not only reduces the aromatic carbon concentration per unit mass but also introduces flexibility into the rigid epoxy structure. This dilution and structural modification are reflected in the shifting NMR signal distribution toward the aliphatic region. Literature also supports this interaction, where divalent cations like Mg^{2+} promote silanol-epoxy condensation through intermediate complexation or catalytic stabilization [67, 68] Mg^{2+} may also temporarily bond with oxygen atoms in both PDMS and the epoxy, which would stabilize transition states and lower the energy needed to form bonds. This mechanism, previously reported in polymer–inorganic hybrid literature, aligns with the observed structural trends [69-71]. Figure 4 illustrates this mechanism, highlighting the stepwise process: $Mg(OH)_2$ releases OH^- ions that open the epoxy ring, and the resulting alkoxides react with PDMS-OH to form covalent.

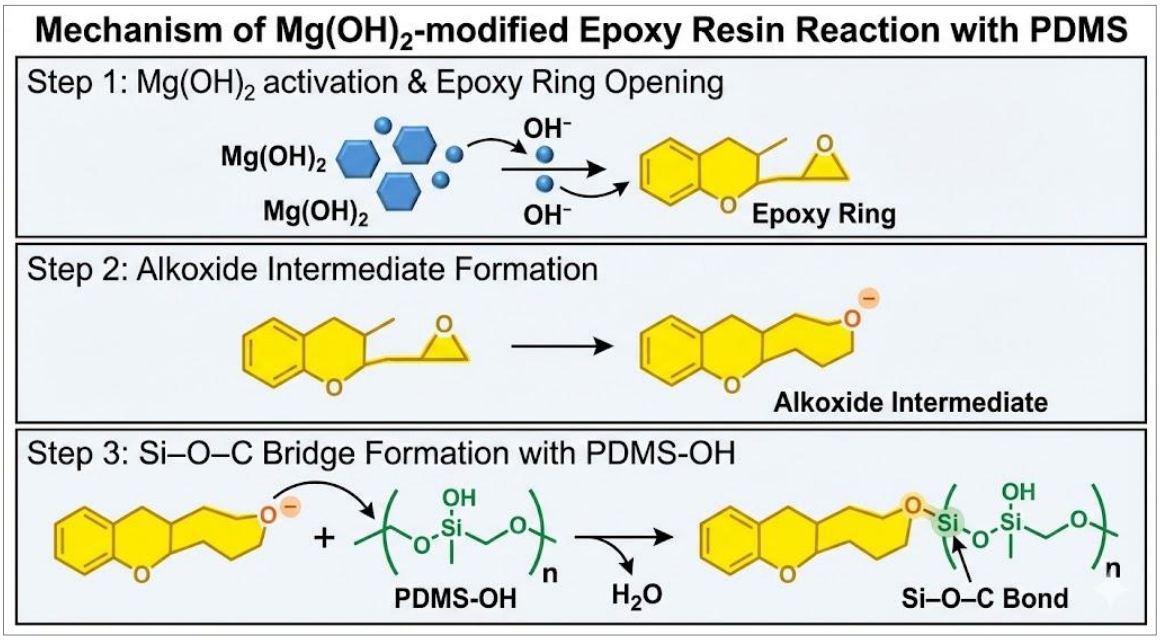

Figure 4. Proposed reaction mechanism illustrating $Mg(OH)_2$-assisted epoxy ring opening and subsequent formation of siloxane–epoxy (Si–O–C) linkages during epoxy resin modification, leading to an altered polymer network structure

The final product is a semi-interpenetrating hybrid network composed of covalently linked siloxane and epoxy phases, with dispersed $Mg(OH)_2$. This hybrid structure preserves partial aromaticity and thermosetting ability while benefiting from enhanced flexibility and thermal performance due to the PDMS and Mg content. FTIR analysis has supported the formation of Si–O–C and Si–O–Mg bonds, corroborating the NMR-based mechanism. Table 3 summarizes

the quantitative changes in aromatic signal intensities, reinforcing the proposed reaction pathway. A reduction in aromatic carbon intensity upon siloxane introduction has also been documented in recent hybrid epoxy systems. Past research reported a 40–60% decrease in aromatic resonance when PDMS was chemically tethered to DGEBA, attributing this to partial disruption of the aromatic environment and shielding effects from flexible siloxane chains. The decreasing aromatic signal strength in MER-1 to MER-5 strongly supports these previous mechanistic interpretations [61, 72, 73].

Figure A-2 further supports this interpretation, clearly showing the progressive decline in aromatic carbon signals with increasing PDMS content. Based on these insights, the reaction mechanism proposed in Figure 4 is strongly validated. XRD analysis, discussed in later sections, provides additional evidence confirming this structural evolution. Overall, the integration of PDMS into BPA epoxy resin through $Mg(OH)_2$-mediated epoxy ring-opening and silanol condensation establishes a novel hybrid binder system with potential application in advanced intumescent fire-retardant coatings.

In the uncured modified resins, PDMS is primarily dispersed and interacts with the epoxy matrix via physical interactions, hydrogen bonding, and coordination to $Mg(OH)_2$, leading to changes in the local electronic environment detectable by ^{13}C NMR. Epoxy chemistry proceeds predominantly via epoxide ring opening, which generates hydroxyl groups on the polymer backbone. On thermal curing or heating with intumescent additives, these hydroxyl groups can condense with silanol (Si–OH) groups associated with PDMS (or silanol generated in situ), producing Si–O–C linkages. Simultaneously, Si–O–metal and Si–O–P-type interactions may form between siloxane and Mg or P species during thermal treatment. The emergence of these covalent linkages in the cured intumescent coating is supported by the FTIR spectra of cured samples (see Figure 13(b)) and correlates with the observed improvements in thermal stability and char structure.

Table 3. ^{13}C-NMR Analysis of Modified Epoxy Resins

Modified epoxy batches	No. of aromatic peaks	Aromatic carbon (C=C) (δ-ppm)	Signal strength (p.d.u)	Total signal strength of aromatic peaks	% age decrease of aromatic carbon signal strength as compared to MER-0
MER-0	4	156.66	2.82	27.28	-
		143.66	3.14		
		127.79	10.65		
		114.00	10.67		
MER-1	4	155.26	8.51	18.57	31.9%
		142.59	5.52		
		126.72	2.53		
		112.93	2.01		
MER-2	4	155.26	1.41	9.21	66.2%
		142.59	2.01		
		126.72	3.25		
		112.93	2.54		
MER-3	4	155.26	1.03	8.36	69.3%
		142.59	2.06		
		126.72	2.75		
		112.93	2.25		
MER-4	4	157.26	1.31	8.35	69.4%
		142.59	2.10		
		126.72	3.20		
		90.93	2.23		
MER-5	4	159.26	2.10	10.42	61.8%
		142.59	2.81		
		126.72	2.50		
		112.93	3.01		

4-4- Thermal Stability Analysis of Modified Epoxy Resins

The Differential Scanning Calorimetry (DSC) thermograms (Figure 2(b)) provide a comparative thermal analysis of a base epoxy resin (MER-0) and a modified epoxy resin (MER-3), which incorporates 30 wt% hydroxyl-terminated polydimethylsiloxane (PDMS) and 2 wt% magnesium hydroxide ($Mg(OH)_2$). As observed in the thermograms, MER-0

exhibits a significant exothermic event around 140°C, indicating the onset of degradation in the unmodified bisphenol A-based epoxy resin. This behavior is characteristic of thermally labile epoxy networks that degrade via scission of ether linkages and ring opening of unreacted oxirane groups. In contrast, MER-3 shows a major degradation peak shifted to approximately 350°C, suggesting a substantial enhancement in thermal stability.

The improved thermal stability in MER-3 can be attributed to a synergistic interaction between PDMS and $Mg(OH)_2$ within the epoxy network, resulting in both chemical grafting and physical reinforcement: $Mg(OH)_2$ functions as a mild Lewis base catalyst, facilitating the condensation reaction between hydroxyl-terminated PDMS and epoxide rings of the epoxy resin. This leads to the formation of Si–O–C linkages, effectively grafting PDMS chains into the resin matrix and forming a semi-interpenetrating polymer network (SIPN). The integration of flexible siloxane chains restricts segmental mobility and improves thermal resistance through covalent bonding [71].

Additionally, Mg^{2+} ions are reported to catalyze epoxide ring-opening reactions by stabilizing alkoxide intermediates, thereby enhancing condensation between silanol and epoxide groups [74]. PDMS possesses a highly stable -Si–O–Si- siloxane backbone, known for its thermal oxidation resistance and high decomposition temperature (>400 °C) [69]. When grafted into the epoxy matrix, PDMS introduces thermal buffering capacity and improves energy dissipation during heating. This modification also reduces internal stresses and delays thermal scission by increasing chain flexibility. Even at low loading (2 wt%), $Mg(OH)_2$ nanoparticles can act as physical barriers to heat transfer and promote char formation. Upon decomposition, $Mg(OH)_2$ releases water vapor, which may slightly cool the matrix and dilute volatile degradation products, contributing further to thermal delay [70]. This heat sink effect complements the chemical stabilization offered by PDMS. The DSC results clearly show that MER-3 possesses superior thermal stability compared to MER-0, with a major degradation event delayed by over 200 °C (from 140 °C to 350 °C). This improvement is directly linked to the formation of Si–O–C bonds, the thermal buffering effect of PDMS, and the catalytic action of $Mg(OH)_2$. These findings confirm that even without intumescent additives, the binder system itself has been thermally stabilized—an essential prerequisite for high-performance intumescent fire-retardant coatings (IFRCs). This concludes the discussion of results conducted in Section 3.1, which explicitly demonstrates the successful chemical integration of siloxane segments within the epoxy matrix, leading to significantly enhanced thermal stability of the modified epoxy systems. The pivotal role of magnesium hydroxide ($Mg(OH)_2$) in facilitating the ring-opening of the epoxide functionalities, thereby enabling the grafting of hydroxyl-terminated PDMS chains, has been established. The formation of stable Si-O-C linkages, critical for this enhanced thermal performance, has been validated through Fourier Transform Infrared (FTIR) spectroscopy, providing molecular-level evidence of the successful reaction.

Furthermore, rheological characterization indicated that the viscosities of MER-3 and MER-4 remain within a suitable range for the effective incorporation of intumescent ingredients. While MER-5 exhibited a significant increase in viscosity, rendering its processing more challenging, preliminary coating samples were nevertheless prepared to explore its fire-retardant properties. This systematic evaluation, despite the processing difficulties, was undertaken to comprehensively assess the performance across the range of modified epoxies. The following section will investigate the fire testing analyses conducted on the intumescent coating samples prepared using these modified epoxy resins, examining their impact on fire resistance phenomena. Accordingly, while FTIR provides limited direct evidence due to spectral overlap, the formation of siloxane–epoxy linkages is more reliably supported by the ^{13}C NMR and DSC analyses, which are more sensitive to changes in the local chemical environment and network structure

4-5- Fire Protection Analysis of IFRCs Developed with Modified Epoxy Resins

4-5-1- Furnace Test (ISO-834)

To evaluate the fire protection capability of the modified epoxy resin systems, all batches were used to develop intumescent fire-retardant coating (IFRC) formulations as described in Section 2.3. Char expansion and morphology were assessed by subjecting the coated steel plates to a furnace test at 800°C according to ISO 834 standards using a Carbolite furnace. The coatings were allowed to cure at room temperature for 24 hours prior to testing. The formulations (IF-0 to IF-5) were developed with increasing concentrations of hydroxyl-terminated PDMS (0–50 wt%) in the modified epoxy resin binder system. Figure 5 presents physical appearances of the post-furnace test appearance of coated samples. Notably, the control formulation (IF-0), which did not contain the modified epoxy binder or any siloxane, exhibited poor char formation. The char residue of IF-0 was brittle, fragmented, and non-continuous, primarily due to the absence of silicon and magnesium-silicate-containing additives that play a key role in thermal stability and char strength. Siloxane incorporation in the resin matrix promotes the development of thermally stable, flexible char due to its ability to form silica-like structures upon combustion.

Furthermore, the presence of magnesium hydroxide [$Mg(OH)_2$] in the resin matrix played a vital role in enhancing char expansion and strength. $Mg(OH)_2$ decomposes endothermically upon heating, releasing water vapor, which dilutes flammable gases and aids in cooling the substrate [75]. Simultaneously, it generates MgO as a ceramic residue, contributing to the reinforcement of the expanded char structure. This mineralization effect enhances the char's mechanical integrity and thermal insulation [76].

In addition, melamine functions as a key blowing agent that decomposes upon heating, releasing non-flammable gases such as ammonia, which facilitates the expansion of the intumescent char. In the current formulations, the combined use of expandable graphite (EG) and pentaerythritol (PER) provides dual carbon sources. This dual-carbon strategy compensates for the reduced aromatic carbon content resulting from the partial replacement of bisphenol A (BPA) with polydimethylsiloxane (PDMS) in the modified epoxy resin [77]. Moreover, the formation of a magnesium silicate network—evident from the FTIR spectra of MER-3, MER-4, and similar formulations—plays a crucial role in enhancing the protective function of the char. This magnesium silicate structure reinforces the char matrix and helps seal micro-pores within it, thereby trapping the gases released by melamine during decomposition [78]. This gas retention contributes to more pronounced expansion, as observed in formulations IF-3 and IF-4, which exhibited higher intumescence factors due to the synergistic interaction between melamine, EG/PER, and the magnesium silicate network. Nano alumina, due to its high surface area and thermal conductivity, helps distribute heat uniformly and catalyzes the formation of a stable, compact char. Its nanoscale size allows for efficient interaction with the matrix and gas phase, reinforcing the char and reducing its brittleness.

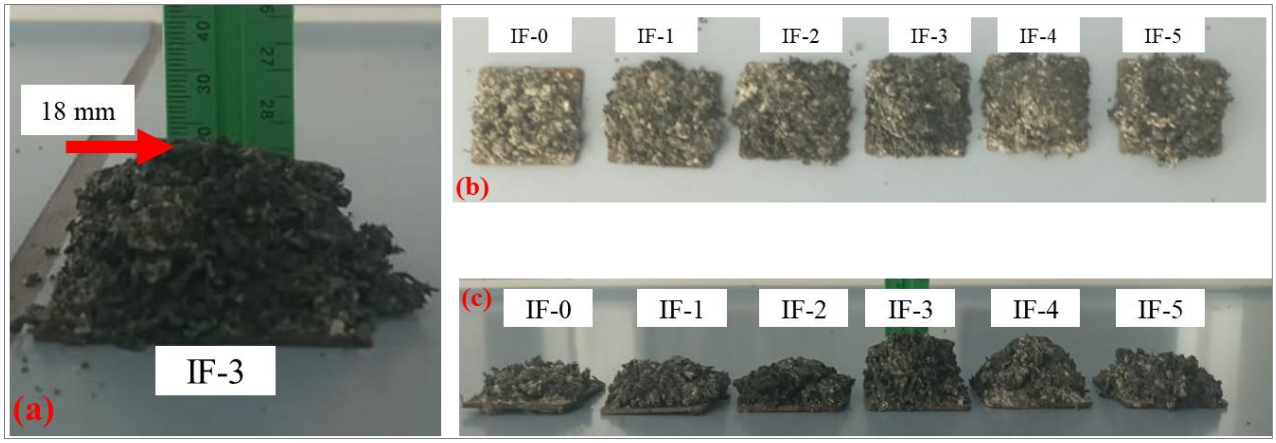

Figure 5. Post-furnace test appearance of coated samples. (a) Close-up of IF-3, showing significant expansion with an approximate height of 18 mm. (b) Bird's-eye view of all samples (IF-0 to IF-5). (c) Side-by-side comparison illustrating the degree of intumescence across the samples, with IF-3 demonstrating the highest expansion.

The intumescence factor (IF), defined as the ratio of the final expanded char thickness (D1) to the original dry coating thickness (D2), was calculated for all formulations and is presented in Table 4 and Figure 4 [79-81]. The IF values are calculated using formula given in Equation 1 and reported in Table 4.

$$Intumescence\ factor\ (IF) = d2/d1 \quad (1)$$

where, $d2$ = Final thickness of the expanded char after furnace testing (mm); and $d1$ = Initial dry thickness of the coating before testing (mm).

Table 4. Char Expansion Data for IFRC Formulations based on $Mg(OH)_2$-Dispersed Modified Epoxy

Formulation	*d1 (mm)*	*d2(mm)*	Intumescence Factor (IF)
IF-0	3.32	10.00	3.01
IF-1	3.25	13.00	4.00
IF-2	2.90	13.20	4.55
IF-3	2.88	17.50	6.08
IF-4	2.96	16.00	5.41
IF-5	3.14	14.00	4.46

As the amount of PDMS increased from IF-0 to IF-3, the intumescence factor also increased. This means that gas evolution and char-forming behavior improved because heat was better distributed and the polymer was more fluid. The combination of PDMS with $Mg(OH)_2$ and synergistic EG/PER/nano alumina in IF-3 led to the highest char expansion (IF = 6.08), suggesting a highly efficient intumescent system. For each 5 × 5 cm coated steel plate, char thickness was measured at five points placed at equal distances: one at the center and four at the corners. Thickness was recorded at

the same positions before and after the ISO-834 furnace test, and the expansion ratio was calculated using the average of these five measurements. This method minimizes errors caused by localized char collapse or nonuniform swelling (see Figure A-3). However, in the case of IF-5 (50% PDMS), the char expansion declined. This can be attributed to the excessive siloxane content, which, while thermally stable, lacks sufficient carbon content needed for effective char formation [18]. A high siloxane ratio dilutes the carbon-rich epoxy segments and restricts char continuity, resulting in a weaker and less expanded residue [51]. These results confirm that a balanced formulation containing $Mg(OH)_2$, optimized PDMS content, and synergistic additives like EG, PER, and nano alumina leads to superior fire retardant performance, as evidenced by improved char quality and higher expansion ratios.

4-5-2- Fire Test (ASTM E119 Standard Test Method)

To assess the fire protection capability of the developed intumescent coatings, a direct flame exposure test was conducted following the ASTM E119 protocol. The setup involved exposing coated steel substrates to a high-intensity butane torch flame (≈3300°C) under controlled conditions. At the same time, thermocouples measured the backface temperatures in real-time, as shown in Figure 6. This test simulates a controlled fire exposure by subjecting coated steel substrates to fire. The test measures the back-face temperature of the substrate over time to assess the coating's effectiveness in insulating and protecting the underlying steel substrate from heat.

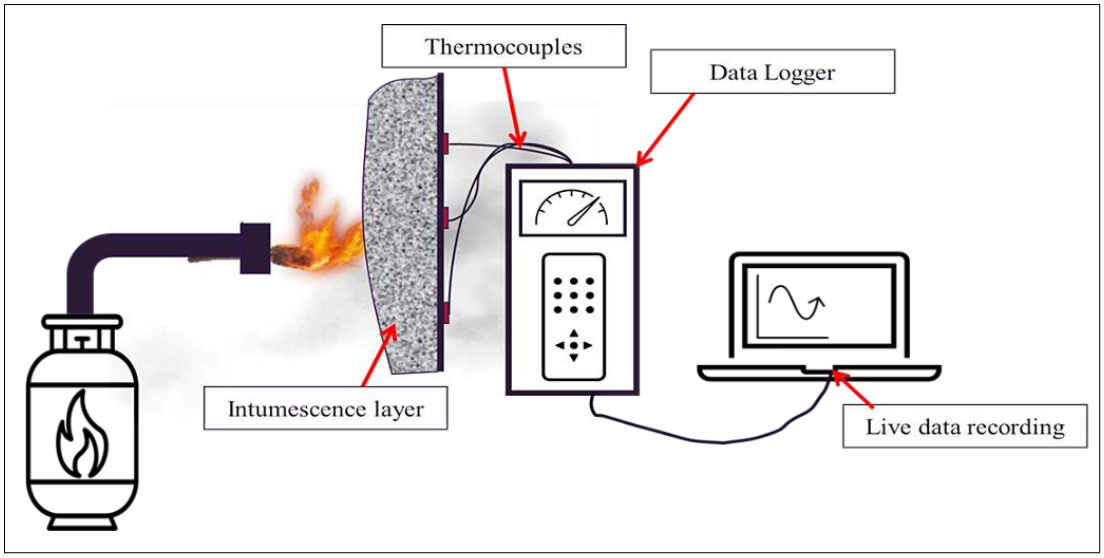

Figure 6. Set up illustration for real-time data acquisition during an ASTM E-119 fire test on an intumescent coating. Thermocouples monitor temperature progression as the reactive layer expands, providing quantitative performance metrics

Each formulation was tested using three independent coated steel samples. The backside temperature measurements showed a variation of ±6–10°C across replicates, and the plotted curves represent the average of these three runs. In all exposed samples, an initial sharp rise in back-face temperature was observed as the flame directly impacted the surface. However, as the temperature increased, the intumescent phenomenon was activated, leading to the formation of a spongy, expanded char barrier. This insulating layer effectively slowed further heat transfer, helping to stabilize and sustain the temperature on the backside of the steel substrate, as shown in Figure 7(a). The baseline sample (IF-0), prepared with traditional epoxy resin without siloxane, showed the highest back-face temperature of 370°C, indicating poor insulation and rapid heat transfer. Upon incorporation of hydroxyl-terminated PDMS into the epoxy system, a consistent reduction in back-face temperature was observed. IF-1 and IF-2, containing 10% and 20% siloxane, respectively, demonstrated improved fire resistance, with recorded temperatures of 331°C and 303°C.

Although siloxane-based materials have previously been used to modify BPA epoxy and magnesium compounds have been employed as fillers in earlier studies [56, 58, 61, 72, 82-84], this work introduces a fundamentally different approach. In the present study, BPA epoxy was first dispersed with magnesium species and subsequently modified with siloxane, creating a dual-doped system that has not been explored before. This combination of Mg and siloxane makes it possible to create new thermally stable hybrid phases that greatly improve fire performance. The cooperative presence of Mg-derived silicates and siloxane-derived Al- and P-rich species promotes pore blocking, strengthens the condensed-phase structure, and contributes to more effective entrapment of toxic gases during decomposition.

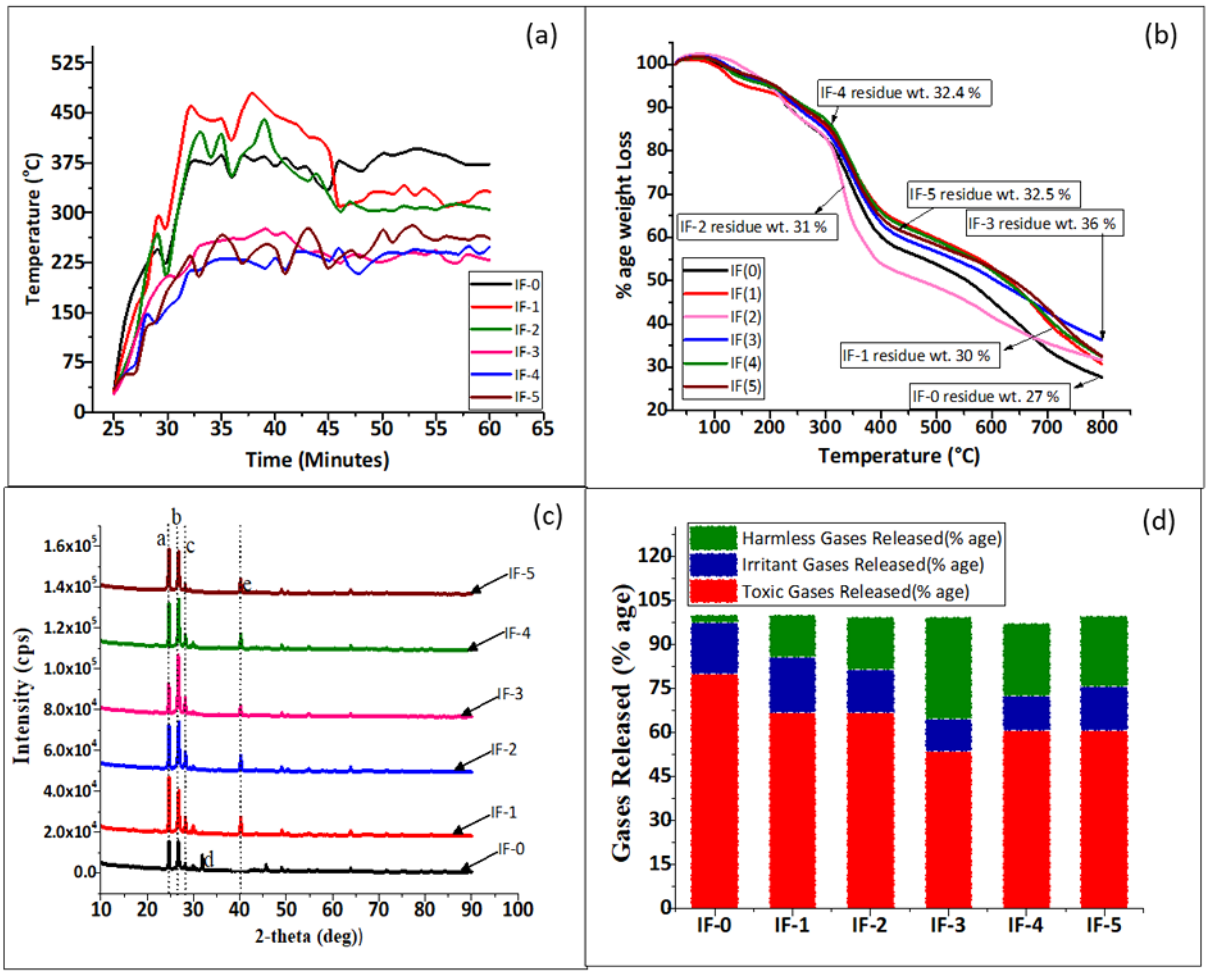

Figure 7. Consolidated analysis of modified epoxy–based intumescent fire-retardant coatings (IFRCs). (A) Fire test (ASTM E-119) showing backside temperature profiles of coated steel substrates over time. (B) Thermogravimetric analysis (TGA) curves displaying thermal degradation and char residue percentages up to 800 °C. (C) X-ray diffraction (XRD) patterns of post-burn char residues, indicating crystalline phases formed during combustion. (D) Gas chromatography–mass spectrometry (GC–MS) analysis of evolved gases, classifying emissions into toxic, irritant, and harmless categories.

The most notable performance was achieved by IF-3, containing 30% siloxane-modified epoxy, which reduced the back-face temperature to 227°C. This significant improvement reflects the formation of a compact and thermally stable char, as well as enhanced gas-barrier effects attributed to siloxane domains and their conversion to a silica-like residue during combustion. However, increasing the siloxane content beyond 30% adversely affected the coating's fire resistance and adhesion. IF-4 and IF-5 showed back-face temperatures of 250°C and 261°C, respectively. These higher values were associated with partial detachment of the coatings from the substrate during testing, attributed to the lubricating or oily nature of excess PDMS, which reduces mechanical bonding and film integrity. These findings suggest that while siloxane incorporation enhances thermal stability and fire performance, excessive amounts compromise adhesion. Therefore, IF-3 (30% PDMS) was identified as the optimal formulation, striking the best balance between thermal insulation and coating integrity. Fire resistance can be further enhanced by fine-tuning the siloxane concentration and incorporating reinforcing fillers such as alumina or nanoclays to improve char strength and structural cohesion during fire exposure. Figure A-4 shows sample IF-3 coated samples before and after the fire test.

4-5-3- Char Morphology Analysis of IFRCs Developed with Modified Epoxy Resins

Scanning Electron Microscopy (SEM) micrographs provided significant insights into the morphology of char residues formed after combustion of the intumescent fire-retardant coatings (IFRCs) based on modified epoxy systems. In the control sample, IF-0, which lacked siloxane modification, the char structure appeared highly porous and disordered, with loosely connected carbonaceous fragments and evident structural collapse (see Figure 8). The SEM image of IF-0 reveals an open-pored, loosely packed char structure with large voids that allow the escape of pyrolysis gases, resulting in a fragile and less effective barrier. In contrast, IF-3 exhibits a much denser and spongier char with predominantly closed and blocked pores. This transformation is attributed to the formation of a robust Mg–Al–silicate network during combustion, which reinforces the char, enhances structural cohesion, and improves its insulating

properties. The compact char structure in IF-3 not only impedes the ingress of heat and oxygen but also effectively traps volatile degradation products, contributing to enhanced fire retardancy. This morphology suggests that the unmodified resin system failed to generate a continuous barrier during thermal degradation, leading to higher flammability and less efficient protection. The porous nature of the char allows for easy escape of pyrolysis gases and ingress of oxygen, which promotes further degradation; a phenomenon also observed in earlier studies on unreinforced IFRCs [85].

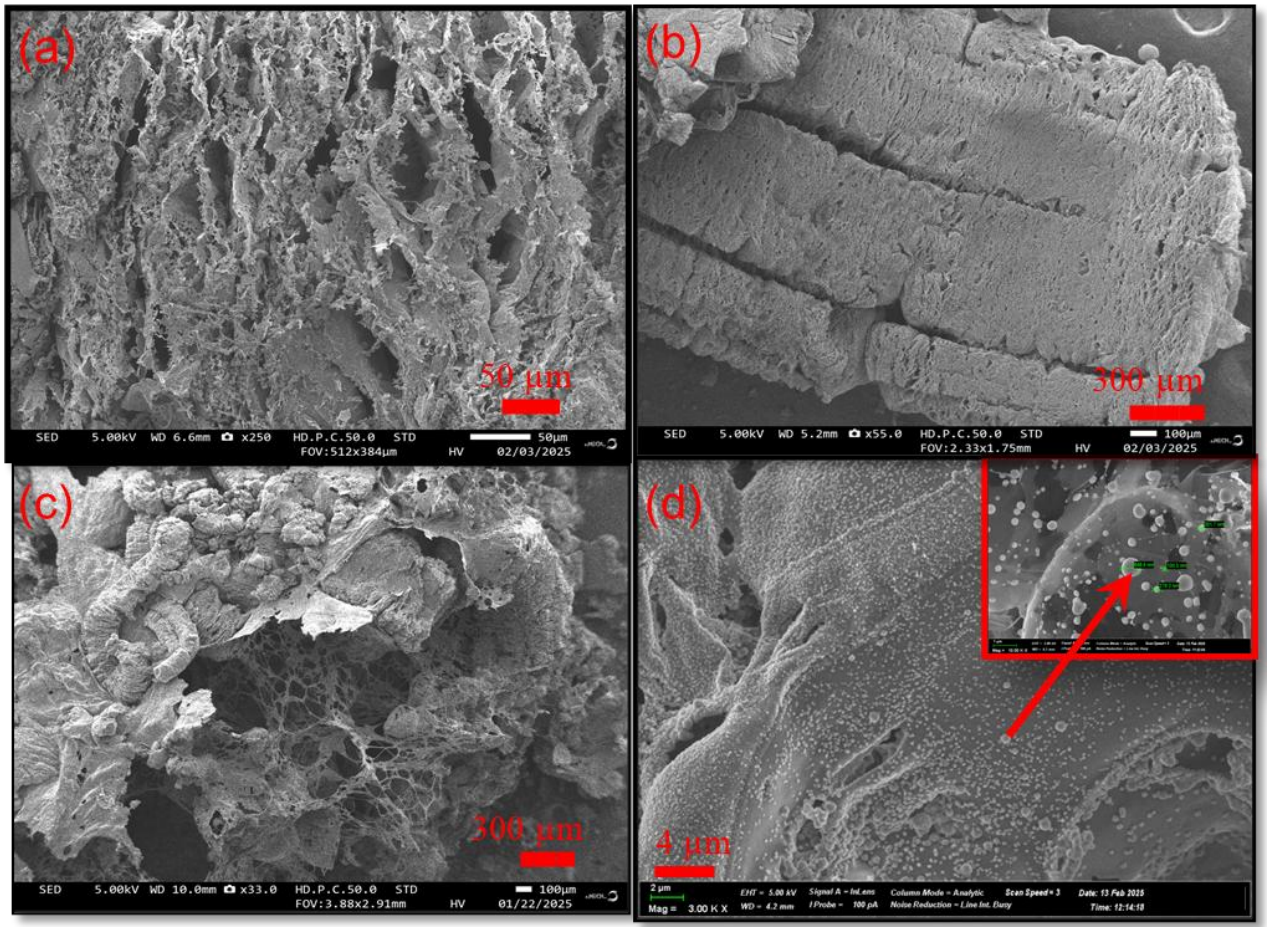

Figure 8. SEM images comparing char residues of IF-0 (a, c) and IF-3 (b, d). The IF-0 sample exhibits a porous and fragile structure, while IF-3 shows a compact, closed-pore morphology attributed to the formation of a Mg–Al–silicate network. The absence of siloxane in IF-0 (c) contrasts with the uniform surface coverage of siloxane-rich particles observed in IF-3 (d).

It was observed in the morphology of IF-3, which incorporated 30 wt% hydroxyl-terminated polydimethylsiloxane (PDMS). The char layer had a solid and coherent structure, with spherical nanoparticles that were tightly packed and evenly spread out across the surface. A high-magnification inset confirmed the successful anchoring of siloxane-derived nano-domains, ranging from ~100 to ~300 nm in size, suggesting effective dispersion of siloxane during the thermal decomposition process. This dense nanoparticle coverage contributes to multiple flame-retardant functions. Firstly, it enhances the barrier effect by reducing pore size and increasing tortuosity, thus obstructing the transport of volatile degradation products and oxygen through the char layer [86]. Secondly, the presence of siloxane reinforces the char's foam-like structure, stabilizing it against collapse. The inorganic siloxane framework likely stiffens the cellular walls within the intumescent char, leading to enhanced mechanical integrity even at elevated temperatures [42].

The SEM analysis reveals a clear distinction between the microstructures of IF-0 and IF-3. IF-0 exhibits a fragile, open framework composed of loosely bound inorganic residues, with no presence of siloxane, resulting in poor char cohesion and limited barrier functionality. In contrast, IF-3 presents a compact, smooth char surface densely decorated with uniformly dispersed siloxane-rich particles, as highlighted in Figure 9. This uniform siloxane attachment significantly enhances the char's mechanical strength and thermal shielding capability. Moreover, even the distribution of nano-alumina and magnesium silicate particles in IF-3 promotes the development of a hybrid ceramic-like protective layer. These inorganic networks work synergistically with the siloxane matrix to form a robust, thermally stable barrier. The formation of alumina and magnesium silicate phases is a well-established strategy for improving fire resistance, as these compounds contribute to thermal insulation and reduce the permeability and structural degradation of the char [87]. The role of these silicates is evident in the denser, smoother surface observed in IF-3 compared to IF-0, supporting the hypothesis that inorganic filler particles and siloxane collaboratively enhance char quality.

IF-4 also displayed a relatively compact char morphology, although slightly less uniform than IF-3. The distribution of particles was less dense, and some pore formation was still visible. This suggests that 40 wt% siloxane may lead to diminishing returns due to partial phase separation or viscosity-related issues during mixing, which can hinder uniform filler dispersion. Nonetheless, the overall improvement in char integrity compared to the unmodified IF-0 was evident. In contrast, IF-5, which contained 50 wt% siloxane, revealed excessive particle accumulation and agglomeration across the char surface, as shown in Figure 9. While the presence of nano-domains was confirmed, their overabundance appeared to compromise the continuity of the barrier. SEM images showed clusters of spherical particles, some exceeding 400 nm in size, with poor interconnection and voids between them. Excess siloxane likely led to particle coalescence during the combustion process, resulting in a brittle and less cohesive char structure. Such observations align with previous findings that excessive siloxane content can reduce char uniformity and introduce thermomechanical weaknesses [88]. Hence, while siloxane significantly improves flame-retardant behavior at optimal levels, overloading leads to reduced efficiency due to agglomeration and phase instability.

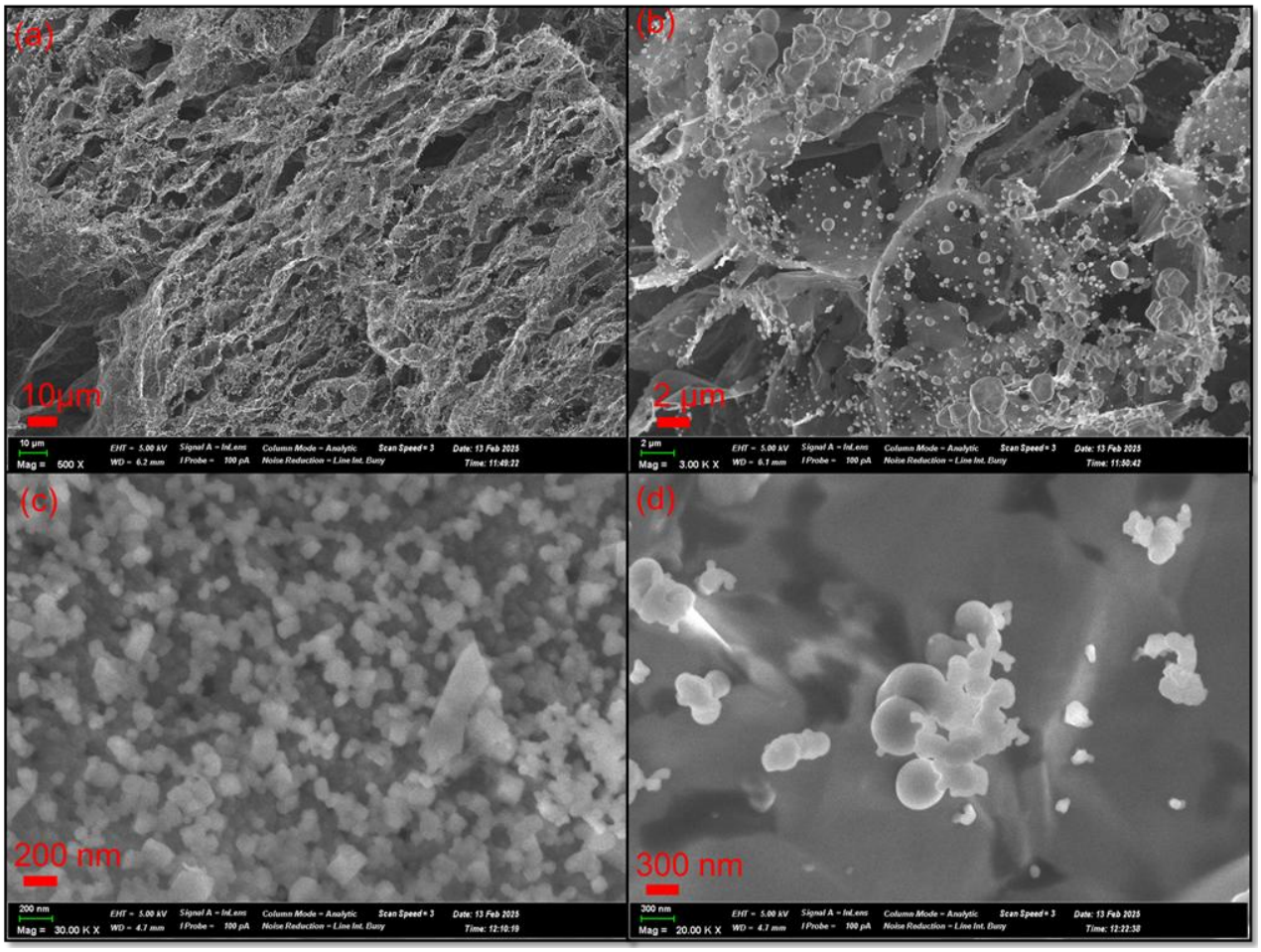

Figure 9. SEM images of IF-4 (a, b) and IF-5 (c, d) char residues showing a progressive increase in siloxane content, with IF-5 displaying pronounced accumulation and agglomeration of siloxane-rich particles across the char surface

These morphological trends affirm the critical role of siloxane in improving IFRC performance. Its multifunctionality; ranging from barrier formation to foam stabilization, gas-phase adsorption, and thermal protection; makes it a highly effective additive in advanced fire-retardant coatings. IF-3 emerges as the most optimized formulation, where the synergistic action of siloxane, nano-alumina, and magnesium oxide resulted in a structurally intact, continuous, and tightly packed char layer capable of enduring high thermal flux. Although previous studies have indicated that intumescent systems commonly develop multicellular char structures, most of those works were carried out using either conventional epoxy binders or single-component inorganic additions. In contrast, the present system demonstrates a distinctly denser and more cohesive morphology, which appears to arise from the simultaneous presence of Mg-based species and siloxane-rich phases. Earlier reports on standard APP–melamine–char systems describe relatively open and brittle char frameworks, whereas the micrographs obtained in this study show tighter pore walls and improved structural continuity [19, 35, 39, 45, 47]. This indicates that the binder modification strategy employed here produces a unique condensed-phase architecture that has not been documented in prior formulations.

Figures 10(a) and 10(b) present the proposed mechanism of heat and fire resistance in the modified epoxy resin, illustrating suppression of toxic volatiles, aromatic breakdown stabilization by PDMS, and reinforcement through $Mg(OH)_2$ and Al_2O_3 leading to the formation of Si–O–C, Mg–Si–O, and Al–Si–O composite networks and the Energy-Dispersive X-ray Spectroscopy (EDS) mapping of the IF-3 intumescent coating, which was formulated using MER-3 resin containing 30 wt% hydroxyl-terminated polydimethylsiloxane (PDMS). The layered EDS image (Figure 10(b) left) visually confirms the uniform dispersion and successful incorporation of siloxane structures within the char matrix. The presence of silicon (Si, purple) is particularly prominent, suggesting effective interaction of PDMS with the epoxy resin matrix and its contribution to the formation of a thermally stable silicate network upon combustion. The dense and tortuous morphology observed correlates well with the barrier effect imparted by siloxane, which restricts gas diffusion pathways and promotes char stability during thermal degradation [89].

The elemental maps on the right further confirm the homogeneous distribution of key components. Silicon (Si), aluminum (Al), and magnesium (Mg) signals are distinctly visible across the surface, suggesting the presence of aluminosilicate and magnesium silicate phases. These contribute to structural reinforcement of the char and aid in reducing its porosity. Phosphorus (P) and oxygen (O) maps confirm the retention of ammonium polyphosphate (APP) in the char, while carbon (C) presence is linked to the carbonaceous backbone of the degraded resin. The dispersed magnesium (Mg) and aluminum (Al) indicate synergistic barrier formation, while the Si enrichment highlights the role of siloxane in promoting condensed-phase activity, stabilizing the intumescent foam, and enhancing the overall fire resistance and gas entrapment capability of the coating [90]. Elemental maps reveal widespread dispersion of Al, Mg, Si, P, and O, indicating the formation of aluminosilicate and magnesium silicate networks within the char. These contribute to enhanced barrier properties, improved char integrity, and reduced gas permeability, key factors in the improved flame retardancy of the modified formulation.

4-5-4- Transmission Electron Microscopy (TEM) Analysis

Transmission Electron Microscopy (TEM) analysis was conducted to investigate the microstructural features of the char residue from the IF-3 formulation. The TEM images show that there are nano-aggregates of siloxane-based particles, and that the sizes of the individual particles range from less than 100 nm to about 500 nm. These dimensions confirm that the particles are within the optimal range to effectively interact with the char matrix at the nanoscale, either by physically filling pores or by blocking the diffusion of pyrolysis gases through micro-voids. The high-resolution image on the left (100 nm scale) shows clearly defined spherical inclusions inside the aggregates. The wider view on the right (500 nm scale) shows that these particles are well-dispersed across the char surface (Figure 10c).

The internal structure of these aggregates exhibits a porous or shell-like morphology, characterized by contrast variation within the particles. This indicates a potential core–shell architecture or encapsulation behavior, which is commonly associated with gas adsorption and diffusion barrier formation [91]. Such features are essential in enhancing the protective nature of the char by trapping flammable volatiles and stabilizing the foamed structure during combustion. The presence of multiple voids within the siloxane aggregates also suggests that these particles can act as micro-reservoirs, capable of absorbing gases or interfering with their movement through the matrix, thereby contributing to reduced flammability and smoke toxicity [92].

Furthermore, the uniform dispersion of these nano-aggregates in the polymer matrix implies good interfacial compatibility between the siloxane domains and the surrounding epoxy network. This functionality is likely facilitated by the hydroxyl termination of PDMS, which improves miscibility and network formation during curing or thermal decomposition [93]. As a result, the siloxane-modified matrix in IF-3 demonstrates improved char cohesion, thermal barrier integrity, and dimensional stability. Together with the EDS analysis, these TEM observations confirm the multifunctional role of siloxane in reinforcing the condensed-phase mechanism of intumescence, thereby improving the fire-retardant performance of the coating.

4-5-5- Results and Discussion of ML Machine Learning-Based Quantitative Analysis of Char Morphology

The trained CNN model achieved a high classification accuracy of 94.2% on the hold-out test set. The detailed performance metrics per class, presented in Table 4, demonstrate the model's robust ability to discern subtle morphological differences. Class D (Dense) showed the highest precision (96%) and recall (95%), indicating the model is exceptionally reliable at identifying the optimal, compact char structure (see Table 5).

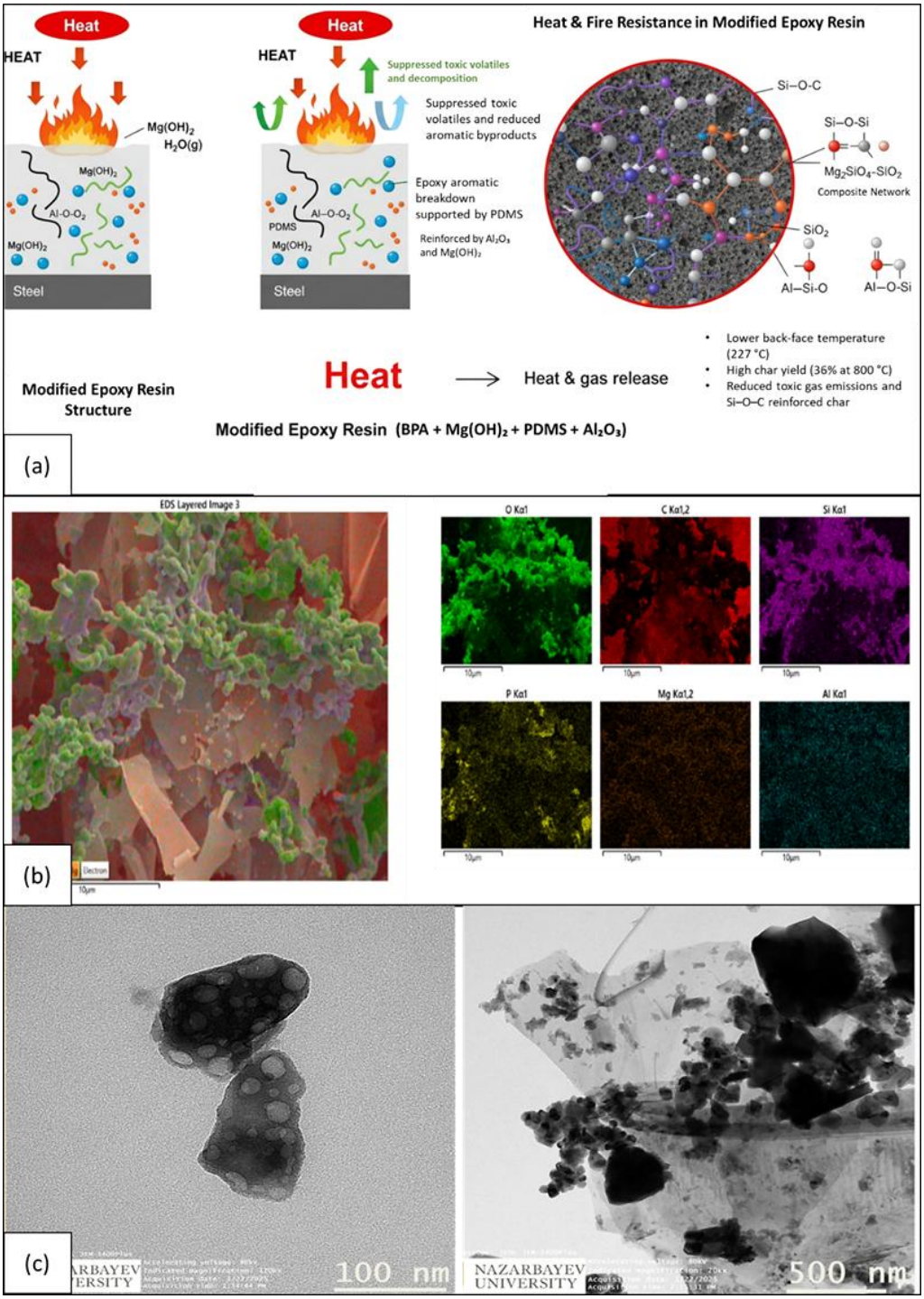

Figure 10. **(a) Proposed mechanism of heat and fire resistance in the modified epoxy resin, illustrating suppression of toxic volatiles, aromatic breakdown stabilization by PDMS, and reinforcement through $Mg(OH)_2$ and Al_2O_3 leading to the formation of Si–O–C, Mg–Si–O, and Al–Si–O composite networks. (b) EDS layered mapping confirming the uniform distribution of Si, Mg, Al, P, O, and C, evidencing siloxane incorporation and bonding interactions within the char structure. (c) TEM micrographs revealing nanoscale porosity and gas entrapment within siloxane-rich domains, demonstrating the role of nano-aggregates in enhancing char compactness and barrier integrity.**

Table 5. **Performance Metrics of the CNN Classifier on the Test Set**

Class	Precision (%)	Recall (%)	F1-Score (%)	Support (n)
Porous (P)	92	93	92.5	36
Dense (D)	96	95	95.5	38
Intermediate (I)	94	94	94.0	34
Overall (Weighted Avg.)	94.3	94.2	94.2	108

The classification probabilities for representative samples from each formulation, as predicted by the model, are presented in Figure 11. The results form a coherent narrative that aligns perfectly with the experimental data: IF-0 was predicted as Class P (Porous) with 98% confidence, consistent with its observed brittle, open-framework morphology. IF-3 was predicted as Class D (Dense) with 96% confidence, confirming its optimal, compact char structure with well-dispersed siloxane-alumina-silicate networks. IF-2 (20% PDMS) and IF-5 (50% PDMS) were both classified with high confidence as Class I (Intermediate), at 82% and 78%, respectively. For IF-2, the classification reflects its transitional state between poor and optimal morphology. For IF-5, this result validates the experimental observation that excessive PDMS leads to agglomeration and a breakdown of the uniform, dense structure, resulting in a sub-optimal, heterogeneous char. A probability heat map (Figure 12) was made to show the classification trends for all formulations. This data provides a clear at-a-glance summary of how the char morphology evolves with increasing PDMS content, culminating in the optimal performance of IF-3 before degrading with over-modification.

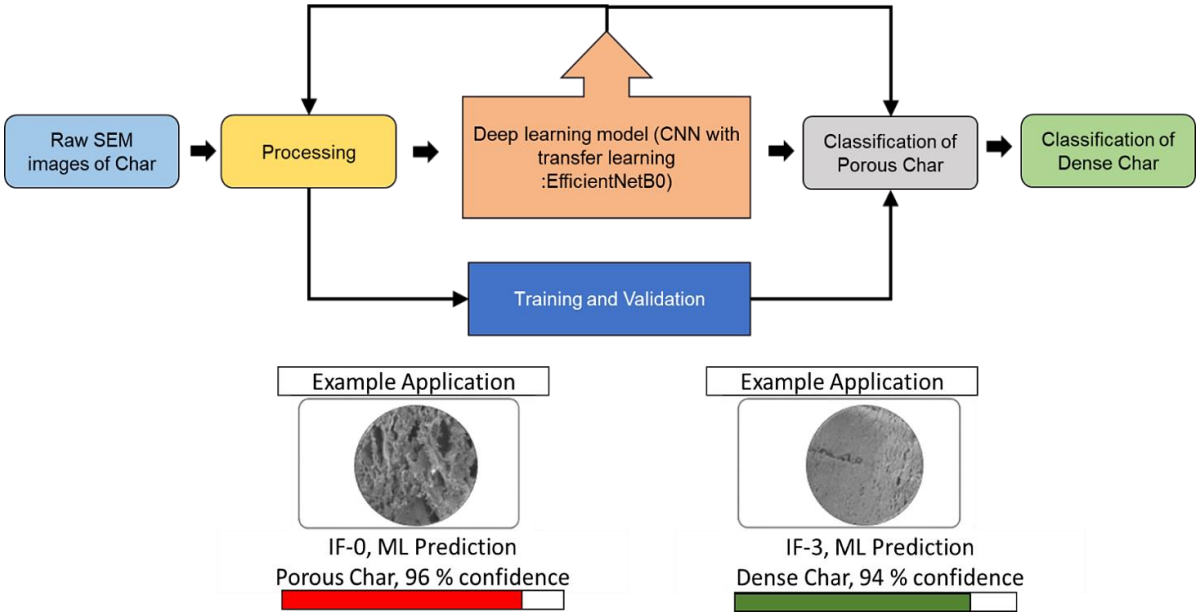

Figure 11. Representative SEM images with ML classification labels and prediction confidence

This machine learning framework successfully transitioned the qualitative description of char morphology into a quantitative, validated classification tool. The high accuracy of the model, corroborated by explainable AI techniques, provides an objective and powerful confirmation of the experimental findings: that a 30 wt.% PDMS loading (IF-3) yields the most superior and consistent dense char morphology. The incorrect classification of IF-5 into the Intermediate class supports the idea that too much siloxane is bad for char uniformity. This approach establishes a precedent for using ML as an integral part of materials characterization in fire science, enabling rapid, automated, and unbiased analysis of microstructural efficacy in next-generation protective coatings.

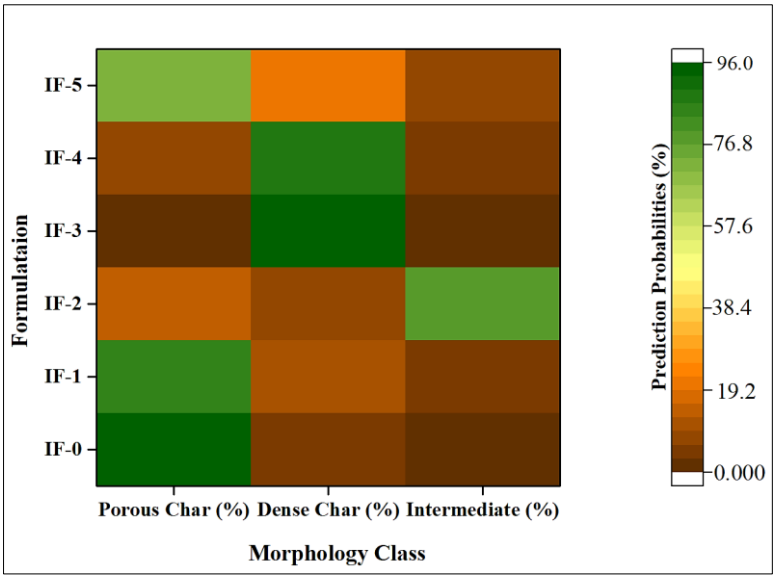

Figure 12. Heat map visualizing the average predicted class probabilities for each IFRC formulation, illustrating the morphological transition with increasing PDMS content

4-5-6- Thermal Stability Analysis (TGA) of Intumescent Coating Formulations

Thermogravimetric analysis (TGA) was performed to assess the thermal degradation behavior and char-forming ability of the intumescent coating formulations (IF-0 to IF-5). The TGA curve (Figure 7(b)) demonstrates that incorporating a modified epoxy resin significantly improves the thermal stability of the coatings. Among all samples, IF-3 exhibited the highest residual weight at 800°C, retaining 36% of its original mass. This high char residue is indicative of improved thermal resistance and the formation of a more stable and protective barrier during combustion. In contrast, the unmodified epoxy-based coating (IF-0) retained only 27% char, underscoring the limited thermal stability of the unreinforced matrix.

The improved performance of IF-3 can be attributed to the synergistic role of $Mg[OH]_2$ and hydroxyl-terminated PDMS within the epoxy matrix. $Mg[OH]_2$ acts as a thermal insulator and promotes the formation of a compact char, while PDMS contributes to the generation of a stable silicate layer that enhances barrier properties in the condensed phase [94]. The siloxane phase, upon decomposition, forms ceramic-like structures such as SiO_2, which further stabilize the char and prevent substrate exposure [95]. This condensed-phase reinforcement reduces the rate of thermal degradation and enhances fire retardancy by increasing the tortuosity of volatile escape paths [96]. Overall, the data suggest that incorporating siloxane-modified epoxy resins improves thermal stability by up to 30% relative to the unmodified system. The TGA residue values for IF-1 through IF-5 (30–36%) highlight the progressive improvement in char yield with increasing siloxane content, with IF-3 representing an optimum formulation. These results are consistent with previous studies that emphasized the importance of condensed-phase activity and char-forming ability in the performance of intumescent fire-retardant coatings.

4-5-7- Differential Scanning Calorimetry (DSC) Analysis of IFRCs

Differential Scanning Calorimetry (DSC) was employed to analyze the thermal transitions and degradation behavior of intumescent fire-retardant coatings (IFRCs) formulated with both unmodified and modified epoxy resins, Figure 13(a). The baseline formulation, IF-0, which was prepared using traditional bisphenol A-based epoxy resin, exhibited a sharp and well-defined exothermic peak in the range of 300°C [97]. This single, intense transition reflects the rapid thermal decomposition of the polyepoxy backbone and suggests limited thermal buffering within the system. Such a concentrated thermal event highlights the lack of structural modifications that could otherwise slow degradation or enhance char-forming mechanisms [98].

In contrast, the DSC thermograms of the PDMS-modified coatings (IF-1 to IF-5) displayed broader decomposition transitions that were slightly shifted to higher temperatures up to 350°C, which shows enhanced thermal stability in IF-1 to IF-5 formulations. This change shows that the thermal degradation process is happening more slowly and in a more controlled way. This is because hydroxyl-terminated polydimethylsiloxane (PDMS) segments were added to the epoxy network. The incorporation of PDMS enhances thermal stability by reducing the rate of polymer breakdown, likely due to its inherent silicon–oxygen backbone, which is more resistant to thermal scission compared to traditional carbon-based epoxy linkages [99]. Additionally, during heating, PDMS is known to generate a silica-like barrier that retards the evolution of volatile degradation products, further stabilizing the system under heat stress. A particularly interesting feature was observed in the derivative thermogravimetry (DTG) profiles of IF-2, where an anomalous increase in the signal occurred between 300 and 400°C. This unexpected rise may result from secondary thermal reactions or transient crosslinking phenomena, where degradation byproducts interact with residual epoxy or siloxane groups, temporarily stabilizing the structure or even increasing mass signal [100].

This phenomenon was more pronounced in formulations with intermediate PDMS content, suggesting a complex interaction between the siloxane segments and the epoxy network. Further investigations, including repeated DSC and DTG measurements, are recommended to eliminate instrumental anomalies and validate this observation [100-102]. The DSC analysis confirms that PDMS incorporation improves thermal buffering and degradation control, which is critical for maintaining intumescence efficiency under fire exposure. $Mg(OH)_2$ fillers and siloxane modifiers have individually been reported to improve the thermal stability of epoxy systems; their sequential incorporation into BPA epoxy—first magnesium dispersion, followed by siloxane modification—has not been explored in prior studies. This engineered dual-doping promotes the formation of Mg-silicate and siloxane-derived inorganic phases that enhance carbonization, delay mass-loss events, and significantly increase residual char. The synergistic interaction between these species yields a thermal stabilization mechanism distinct from conventional intumescent formulations.

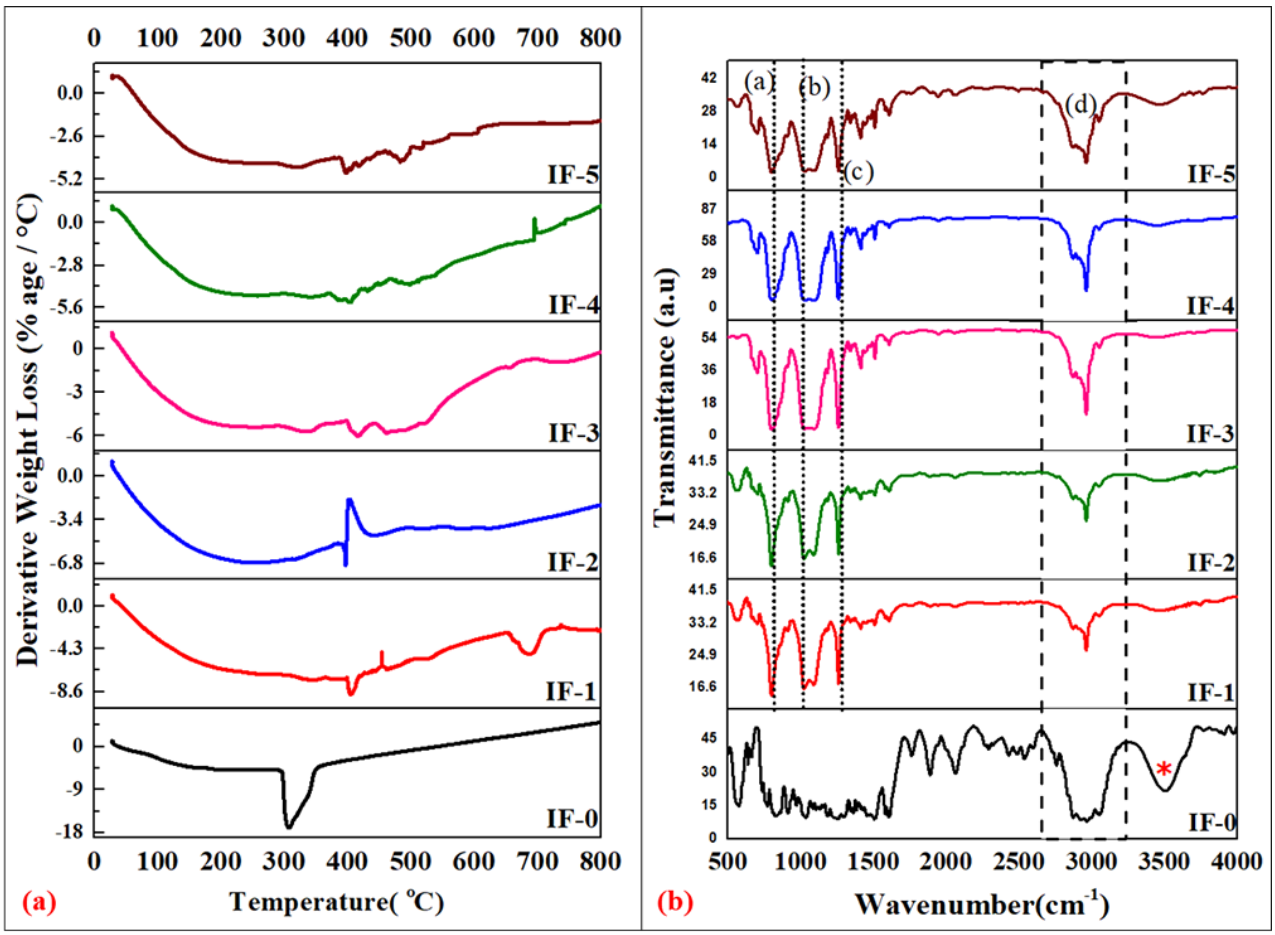

Figure 13. (a) Differential scanning calorimetry (DSC) curves of intumescent fire-retardant coatings (IFRCs) based on modified epoxy resins, illustrating enhanced thermal stability. (b) FTIR spectra of char residues obtained after furnace testing of IFRCs, confirming the formation of siloxane- and phosphate-derived structures in the protective layer.

4-5-8- X-Ray Diffraction (XRD) Analysis of IFRCs

XRD analysis was employed to characterize the crystalline phases formed in the residual char of intumescent fire-retardant coatings (IFRCs) after combustion. Figure 7(c) shows the diffraction patterns of all six formulations (IF-0 to IF-5). The table next to it shows the peaks that were found. These results reveal the evolution of thermally stable inorganic structures that contribute to the integrity and barrier performance of the char layer.

In the unmodified control (IF-0), a notable diffraction peak at 32.7° was attributed to benzo[a]pyrene ($C_{20}H_{12}$), a polycyclic aromatic hydrocarbon generated from incomplete decomposition of bisphenol A–based epoxy resin [103]. This signal was absent in all siloxane-modified samples (IF-1 to IF-5), indicating successful suppression of toxic aromatic byproducts [104]. This observation aligns with ^{13}C NMR findings, which showed a reduction in aromatic carbon content, and with FTIR spectra, where IF-0 exhibited broader and weaker aliphatic C–H stretching vibrations (2950–3000 cm^{-1}), compared to the sharper and more intense peaks in PDMS-modified coatings. These changes reflect a shift toward the saturated carbon structure characteristic of siloxane segments—and support the reduced toxicity and improved thermal behavior of the modified systems [105].

The incorporation of PDMS into the epoxy matrix led to the formation of several high-temperature crystalline phases, notably α-Al_2O_3 (25.6°), BPO_4 (27.8°), $Mg_2P_2O_7$ (28–29°), and forsterite (Mg_2SiO_4, ~40°) (structure given in Figure 14). The presence of forsterite, a thermally stable magnesium silicate phase, confirms the chemical interaction between MgO and PDMS during the combustion process. This finding is further supported by NMR identification of bis(trimethylsiloxy)(1,4-dihydronaphthalene)magnesium (structure given in Figure 9), whose decomposition leads to mineralized forsterite residues [106, 107]. These ceramic-like phases seal pores, reinforce the char matrix, and hinder the release of flammable gases, significantly enhancing fire resistance.

Among all formulations, IF-3 (with 30 wt% PDMS) displayed the most defined and intense crystalline peaks, indicating the most complete transformation into fire-resistant phases. This structural development correlates strongly with TGA results, where IF-3 yielded the highest char residue (36%) and exhibited delayed thermal decomposition [108]. Additionally, the FTIR analysis showed enhanced –OH stretching (3400–3500 cm^{-1}) in modified samples, suggesting increased hydrogen bonding potential and char cohesion. XRD results, interpreted in conjunction with NMR, FTIR, and TGA data, demonstrate that siloxane-modified epoxy coatings facilitate the formation of thermally stable inorganic

networks, suppress toxic residue formation, and produce a mechanically robust and gas-tight char [109]. IF-3 stands out as the optimal formulation, achieving superior crystalline structure, fire protection, and environmental performance. The sequential modification strategy implemented in this study, where Mg dispersion is followed by siloxane incorporation, has promoted the development of new ceramic-like Mg–Si–O and siloxane-associated P/Al phases, which contribute to improved high-temperature stability. Such hybrid crystallization behavior reflects a synergistic phase evolution mechanism absent in conventional formulations and supports the superior fire performance observed in this study.

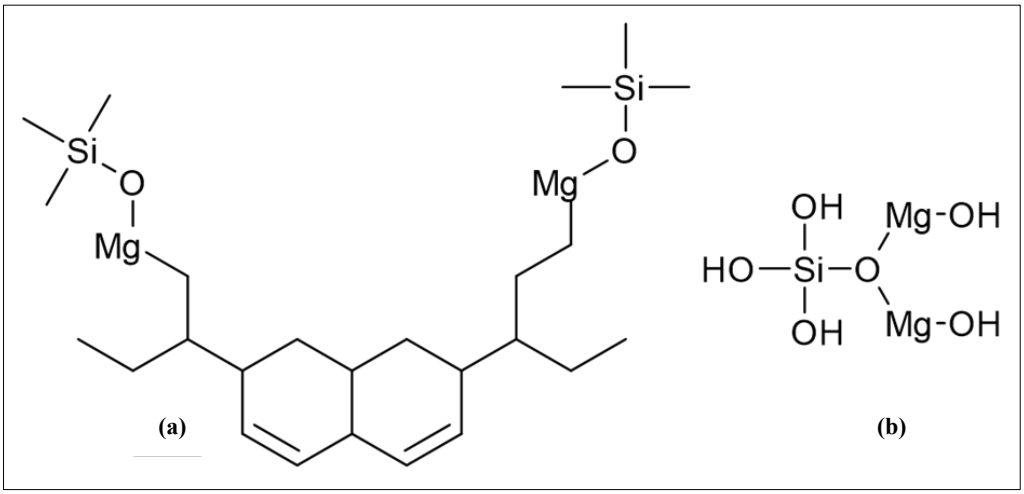

Figure 14. Characterization of ceramic-like phases in the composite char. (a) Chemical structures of α-Al_2O_3, BPO_4, $Mg_2P_2O_7$, and forsterite (Mg_2SiO_4) crystalline phases identified from the XRD pattern of the char residue (b) The molecular structure of a key intermediate, bis(trimethylsiloxy)(1,4-dihydronaphthalene)magnesium, which decomposes to form forsterite.

4-5-9- FTIR Spectroscopy Analysis of IFRCs

FTIR spectroscopy was conducted to investigate the chemical bonding characteristics of both the modified epoxy resin and the char residues obtained after combustion of intumescent fire-retardant coatings (IFRCs). Figure 13(b) illustrates the FTIR spectra for all six formulations (IF-0 to IF-5), highlighting several key peaks associated with siloxane incorporation and post-combustion residue chemistry. In the unmodified reference sample (IF-0), the spectrum lacked distinctive peaks associated with siloxane structures. Specifically, peak (a), which is around 1000–1100 cm^{-1} and corresponds to the asymmetric stretching of Si–O–Si bonds, was not present [110]. This peak, however, was clearly present in all modified samples (IF-1 to IF-5), confirming the successful incorporation of siloxane chains into the epoxy matrix. The peak intensity increased progressively with higher PDMS content, being most prominent in IF-4 and IF-5, indicating stronger crosslinking and more extensive siloxane network formation. Similarly, peak (b) at 1250–1275 cm^{-1}, attributed to Si–CH_3 bending vibrations, appeared only in modified formulations, providing further evidence of methyl-rich PDMS side chains [111]. These methyl groups are known to enhance thermal stability by increasing hydrophobicity and reducing free radical mobility during degradation [47].

Another distinctive feature, peak (c) at 790–810 cm^{-1}, corresponds to Si–C or Si–CH_3 bonds, indicative of covalent bonding between siloxane and the epoxy matrix. The presence of this peak further validates the chemical attachment of siloxane moieties, which plays a critical role in enhancing the gas barrier properties of the coating. Moreover, all siloxane-modified samples exhibited a sharper and more intense aliphatic C–H stretching vibration at 2950–3000 cm^{-1} (peak d), suggesting a higher concentration of saturated carbon atoms [112]. This contrasts with the broader and weaker signal observed in IF-0, typical of unsaturated or aromatic carbon structures. The transition to saturated, non-aromatic configurations in IF-1 to IF-5 aligns with the modification goal of reducing toxic aromatic decomposition products and improving char compactness.

FTIR analysis of the modified epoxy resin confirmed the presence of Si–CH and Si–C bonding; clear signatures of aluminum- or magnesium-related bonding were also observed at this stage. However, FTIR spectra of the post-combustion char residues revealed new bond formations, specifically Si–Mg–C and Si–Al–C linkages [113]. These bands were likely formed during thermal decomposition when MgO and nano-alumina reacted with siloxane-derived species, contributing to a mineralized, ceramic-like char matrix. This transformation complements findings from XRD and NMR analyses, which confirmed forsterite formation and magnesium–silicate bonding. Additionally, a broad –OH stretching band (~3400–3500 cm^{-1}) was more pronounced in siloxane-modified coatings, indicating enhanced hydrogen bonding potential and cohesion in the char layer. FTIR results confirm the successful incorporation of PDMS into the epoxy system and the subsequent formation of chemically stable, thermally resilient networks in the charred residues. These molecular changes contribute significantly to improved flame resistance, reduced toxic emissions, and superior structural performance; especially in IF-3, which consistently displayed the most balanced and well-defined spectral features.

4-5-10- GC-MS Analysis of IFRCs

Gas Chromatography–Mass Spectrometry (GC-MS) was employed to investigate the thermal degradation products of intumescent fire-retardant coatings (IFRCs). In accordance with ISO 13344, evolved gases were classified into three categories—toxic, irritant, and harmless—based on their LC_{50} values [114, 115]. The quantitative breakdown of gaseous emissions is presented in Figure 7(d) and summarized in Table 6.

Table 6. Quantitative Breakdown of Gaseous Emissions in IFRCs Developed with Modified Epoxy Resin

Formulation	Toxic (%)	Irritant (%)	Harmless (%)
IF-0	80.12	17.33	2.55
IF-1	66.63	19.00	14.36
IF-2	66.69	14.78	17.80
IF-3	53.55	10.96	34.90
IF-4	60.84	11.72	24.57
IF-5	60.62	15.13	23.92

The reference sample IF-0, composed of unmodified bisphenol A–based epoxy resin, emitted the highest percentage of toxic gases (80.12%), dominated by aromatic and polycyclic hydrocarbons such as benzo[a]pyrene, a known carcinogen. This result aligns strongly with XRD analysis, where a prominent peak at 32.7° confirmed the presence of this compound in the residual char, suggesting incomplete combustion and a tendency of traditional epoxy to form hazardous aromatic byproducts [116].

In contrast, siloxane-modified formulations (IF-1 to IF-5) exhibited a progressive reduction in toxic gas emissions, with IF-3 standing out by releasing only 53.55% toxic gases and the highest proportion of harmless gases (34.9%). This improvement is attributed to the incorporation of polydimethylsiloxane into the epoxy matrix, which fundamentally alters the degradation chemistry and residue structure of the coating.

NMR analysis validated this transformation, revealing a significant decrease in aromatic carbon signals from IF-1 to IF-5. The absence of benzo[a]pyrene and related species in siloxane-rich samples is further supported by XRD, which confirmed the suppression of aromatic crystalline phases and the emergence of thermally stable mineral phases such as forsterite (Mg_2SiO_4), α-Al_2O_3, BPO_4, and $Mg_2P_2O_7$. These compounds collectively strengthen the residue, reduce volatility, and serve as a ceramic barrier to gas release.

FTIR spectroscopy in Figure 13(b) further substantiates these findings. In IF-1 to IF-5, characteristic peaks at 1000–1100 cm^{-1} (Si–O–Si), 1250–1275 cm^{-1} (Si–CH_3), and 790–810 cm^{-1} (Si–C or Si–CH_3) confirm the successful attachment of siloxane segments into the epoxy backbone [34]. More importantly, post-burn char analysis reveals the development of complex linkages such as Si–Mg–CH and Si–Al–CH, which are indicative of inorganic phase formation during combustion. These networks contribute to a more gas-tight and stable char structure, limiting the escape of toxic degradation products [117].

Additionally, TGA analysis Figure 7(b) supports this mechanism, showing increased residual weight in siloxane-modified coatings, particularly IF-3, which retained 36% char residue. This demonstrates greater thermal resistance and implies a lower release of volatiles; a finding consistent with the decreased toxic gas output observed in the GC-MS analysis.

Although the incorporation of siloxane particles effectively reduced toxic gas emissions, it is important to note that none of the formulations—despite substantial improvements—fully fall within a universally defined ‘safe zone’ in terms of gas toxicity. Therefore, to achieve complete suppression or regulatory compliance, additional strategies such as introducing gas-adsorbing nanofillers and reactive flame-retardant groups, or synergistic additives, should be explored in future formulations. The GC-MS results not only confirm that siloxane-modified epoxy systems can reduce toxicity, but they also match up well with structural and thermal analyses from NMR, FTIR, XRD, and TGA. Among all the formulations, IF-3 emerges as the most environmentally responsible and fire-resilient coating, offering a promising route toward safer, high-performance IFRCs.

Most previously published GC–MS analyses for intumescent coatings focus on identifying common volatile fragments originating from APP degradation, melamine deamination, or aromatic species released from unmodified epoxy resins. These studies generally report typical signatures of small nitrogen compounds and phenolic fragments associated with conventional epoxy breakdown [73, 118, 119]. In contrast, the present formulation exhibits a markedly different distribution of evolved species, with substantially reduced aromatic by-products and a shift toward more oxidized or cross-linked fragments. Such a profile is consistent with the combined influence of Mg-containing intermediates and the siloxane-modified binder, neither of which has been jointly examined in past GC–MS investigations. This deviation from traditional volatile pathways highlights the distinct degradation mechanism introduced by the dual-modified resin system.

5- Conclusion

This study successfully developed and evaluated siloxane–magnesium hydroxide modified epoxy resins as binder systems for intumescent fire-retardant coatings (IFRCs). By dispersing $Mg(OH)_2$ into bisphenol-A epoxy resin and chemically incorporating hydroxyl-terminated PDMS, a hybrid resin network with enhanced thermal stability and reduced toxicity was achieved. The modified resins demonstrated improved chain flexibility, delayed degradation, and formation of stable Si–O–C linkages, as confirmed by FTIR, NMR, DSC, and TGA analyses. Among the formulations, IF-3 (30 wt.% PDMS) provided optimal performance, balancing processability and fire resistance. It exhibited superior viscosity control, delayed degradation by more than 200°C compared to the control, and retained the highest char yield (36% at 800°C). Fire testing confirmed that IF-3 produced the most compact and mechanically stable char, reinforced by Si–O–Si, Mg–Si–O–C, and Al–Si–O–Si structures. GC-MS analysis revealed a marked reduction in toxic aromatic emissions and a corresponding increase in harmless gaseous by-products. Furthermore, the application of machine learning to SEM datasets enabled objective, quantitative validation of char morphology, confirming the superiority of IF-3 with over 94% accuracy. The synergistic incorporation of $Mg(OH)_2$ and PDMS not only enhanced the condensed-phase fire protection mechanism but also significantly reduced the release of hazardous volatiles. This scalable, halogen-free approach provides a promising pathway for advancing next-generation epoxy-based IFRCs with improved fire safety, lower toxicity, and compatibility with industrial applications. Future work will focus on further optimization of nanofillers, long-term durability, and large-scale implementation strategies.

6- Declarations

6-1- Author Contributions

Conceptualization, A.M.; methodology, A.M.; software, M.F.J.; validation, M.F.J.; formal analysis, Q.F.G.; investigation, Q.F.G.; resources, S.K.; data curation, Q.F.G.; writing—original draft preparation, Q.F.G.; writing—review and editing, Q.F.G.; visualization, Q.F.G.; supervision, A.M.; project administration, S.K.; funding acquisition, S.K. All authors have read and agreed to the published version of the manuscript.

6-2- Data Availability Statement

The data presented in this study are available in [https://doi.org/10.5281/zenodo.19449819] and [https://colab.research.google.com/drive/1inMGHU2nMsXcsO6A4D21i4eR90fNWnhJ?usp=sharing].

6-3- Funding and Acknowledgments

The authors acknowledge the financial support provided by FDCRGP-040225FD4739 and the research facilities provided by the Department of Chemical Engineering, Nazarbayev University, Kazakhstan. The authors also thank the laboratory staff for their technical assistance during materials synthesis and characterization. Their support contributed substantially to the completion of this work.

6-4- Institutional Review Board Statement

Not applicable.

6-5- Informed Consent Statement

Not applicable.

6-6- Conflicts of Interest

The authors declare that there is no conflict of interest regarding the publication of this manuscript. In addition, the ethical issues, including plagiarism, informed consent, misconduct, data fabrication and/or falsification, double publication and/or submission, and redundancies have been completely observed by the authors.

7- References

[1] Fenimore, C. P. (1975). Candle-Type Test for Flammability of Polymers. Flame-retardant Polymeric Materials, 1975, 371–397. doi:10.1007/978-1-4684-2148-4_9.

[2] Gomez-Mares, M., Tugnoli, A., Landucci, G., Barontini, F., & Cozzani, V. (2012). Behavior of intumescent epoxy resins in fireproofing applications. Journal of Analytical and Applied Pyrolysis, 97, 99–108. doi:10.1016/j.jaap.2012.05.010.

[3] Volkova, N. N., Tarasov, V. P., Erofeev, L. N., & Gorbatkina, Y. A. (2006). The kinetics of thermal degradation and the structure of bisphenol-a epoxy binder modified by active plasticizer. Polymer Science - Series B, 48(2), 96–100. doi:10.1134/S1560090406030109.

[4] Daelemans, L., Van Der Heijden, S., De Baere, I., Muhammad, I., Van Paepegem, W., Rahier, H., & De Clerck, K. (2015). Bisphenol A based polyester binder as an effective interlaminar toughener. Composites Part B: Engineering, 80, 145–153. doi:10.1016/j.compositesb.2015.05.044.

[5] Pimenta, J. T., Gonçalves, C., Hiliou, L., Coelho, J. F. J., & Magalhães, F. D. (2016). Effect of binder on performance of intumescent coatings. Journal of Coatings Technology and Research, 13(2), 227–238. doi:10.1007/s11998-015-9737-5.

[6] Duquesne, S., Magnet, S., Jama, C., & Delobel, R. (2005). Thermoplastic resins for thin film intumescent coatings - Towards a better understanding of their effect on intumescence efficiency. Polymer Degradation and Stability, 88(1), 63–69. doi:10.1016/j.polymdegradstab.2004.01.026.

[7] Mohd Sabee, M. M. S., Itam, Z., Beddu, S., Zahari, N. M., Mohd Kamal, N. L., Mohamad, D., Zulkepli, N. A., Shafiq, M. D., & Abdul Hamid, Z. A. (2022). Flame Retardant Coatings: Additives, Binders, and Fillers. Polymers, 14(14), 2911. doi:10.3390/polym14142911.

[8] Gao, Y. J., Jin, W. J., Hu, B. Q., Cheng, X. W., & Guan, J. P. (2023). Preparation of a Reactive Phosphorus/nitrogen-Based Intumescent Flame Retardant Coating for Cotton Fabrics. Journal of Natural Fibers, 20(1), 2153195. doi:10.1080/15440478.2022.2153195.

[9] Shiu, B. C., Wu, K., Lou, C. W., Lin, Q., & Lin, J. H. (2021). Synthesis of a compound phosphorus-nitrogen intumescent flame retardant for applications to raw lacquer. Polymers, 13(17), 2858. doi:10.3390/polym13172858.

[10] Malkappa, K., Prasad, C., Kang, C. S., Jeong, S. G., Sangaraju, S., Shin, E. J., & Choi, H. Y. (2025). Recent developments of phosphorous–nitrogen-based effective intumescent flame-retardant for polymers and textiles. Polymer Bulletin, 82(11), 5139–5199. doi:10.1007/s00289-025-05689-4.

[11] Gao, X., Shen, J., Sun, Q., Zhang, J., & Sheng, J. (2023). Study on char reinforcing of different inorganic fillers for polyethylene composites. Ceramics International, 49(6), 9566–9573. doi:10.1016/j.ceramint.2022.11.126.

[12] Al-Hassany, Z. (2024). Ceramifiable polymer composites for fire protection application. Doctoral Dissertation, RMIT University, Melbourne, Australia.

[13] Chen, S. N., Li, P. K., Hsieh, T. H., Ho, K. S., & Hong, Y. M. (2021). Enhancements on flame resistance by inorganic silicate-based intumescent coating materials. Materials, 14(21), 6628. doi:10.3390/ma14216628.

[14] Liu, L., Zhang, Y., Li, L., & Wang, Z. (2011). Microencapsulated ammonium polyphosphate with epoxy resin shell: Preparation, characterization, and application in EP system. Polymers for Advanced Technologies, 22(12), 2403–2408. doi:10.1002/pat.1776.

[15] Hu, X., & Sun, Z. (2021). Nano CaAlCO3-layered double hydroxide-doped intumescent fire-retardant coating for mitigating wood fire hazards. Journal of Building Engineering, 44, 102987. doi:10.1016/j.jobe.2021.102987.

[16] Xu, Z., Deng, N., & Yan, L. (2020). Flame retardancy and smoke suppression properties of transparent intumescent fire-retardant coatings reinforced with layered double hydroxides. Journal of Coatings Technology and Research, 17(1), 157–169. doi:10.1007/s11998-019-00249-8.

[17] Hu, X., Zhu, X., & Sun, Z. (2020). Fireproof performance of the intumescent fire retardant coatings with layered double hydroxides additives. Construction and Building Materials, 256, 119445. doi:10.1016/j.conbuildmat.2020.119445.

[18] Gillani, Q. F., Ahmad, F., Mutalib, M. I. A., Megat-Yusoff, P. S. M., & Ullah, S. (2018). Effects of Halloysite Nanotube Reinforcement in Expandable Graphite Based Intumescent Fire-Retardant Coatings Developed Using Hybrid Epoxy Binder System. Chinese Journal of Polymer Science (English Edition), 36(11), 1286–1296. doi:10.1007/s10118-018-2148-1.

[19] Lee, Y. X., Ahmad, F., Kabir, S., Masset, P. J., Onate, E., & Yeoh, G. H. (2022). Synergistic effects of tubular halloysite clay and zirconium phosphate on thermal behavior of intumescent coating for structural steel. Journal of Materials Research and Technology, 18, 4456–4469. doi:10.1016/j.jmrt.2022.04.097.

[20] Banijamali, M. S., Arabi, A. M., Jannesari, A., & Pasbakhsh, P. (2023). Synthesis and characterization of an intumescent halloysite based fire-retardant epoxy system. Applied Clay Science, 241, 106995. doi:10.1016/j.clay.2023.106995.

[21] Zhang, Q., Shu, Y., Zhang, Y., Huo, S., Ye, G., Wang, C., & Liu, Z. (2024). Effect of functionalized halloysite nanotubes on fire resistance and water tolerance of intumescent fire-retardant coatings for steel structures. Progress in Organic Coatings, 197, 108843. doi:10.1016/j.porgcoat.2024.108843.

[22] Yu, J., Guo, C., Wang, J., Song, J., Wang, Y., Cheng, J., Cheng, Y., & Zhang, F. (2024). Preparation of bio-based trinity lignin intumescent flame retardant and its effect on burning behavior and heat transfer process of epoxy resin composites. Progress in Organic Coatings, 195, 108653. doi:10.1016/j.porgcoat.2024.108653.

[23] Zheng, C., Li, D., & Ek, M. (2019). Improving fire retardancy of cellulosic thermal insulating materials by coating with bio-based fire retardants. Nordic Pulp and Paper Research Journal, 34(1), 96–106. doi:10.1515/npprj-2018-0031.

[24] Fan, Z., Li, Y., He, J., Song, B., Chang, M., Fang, X., Yu, L., Yang, G., Guo, H., & Liu, Y. (2025). Bio-based intelligent multifunctional coating for wood: Flame retardancy, fire warning, smoke suppression, thermal insulation and antibacterial activity. Construction and Building Materials, 465, 140244. doi:10.1016/j.conbuildmat.2025.140244.

[25] Wang, X., Nabipour, H., Kan, Y. C., Song, L., & Hu, Y. (2022). A fully bio-based, anti-flammable and non-toxic epoxy thermosetting network for flame-retardant coating applications. Progress in Organic Coatings, 172, 107095. doi:10.1016/j.porgcoat.2022.107095.

[26] Yew, M. C., Yew, M. K., Saw, L. H., Ng, T. C., Durairaj, R., & Beh, J. H. (2018). Influences of nano bio-filler on the fire-resistive and mechanical properties of water-based intumescent coatings. Progress in Organic Coatings, 124, 33–40. doi:10.1016/j.porgcoat.2018.07.022.

[27] Petrović, E. K. (2024). Sustainability and toxicity of polymers, plastics, and coatings in buildings. Sustainability and Toxicity of Building Materials, 2024, 309–333. doi:10.1016/B978-0-323-98336-5.00015-7.

[28] Celiński, M., & Sankowska, M. (2016). Explosibility, flammability and the thermal decomposition of Bisphenol A, the main component of epoxy resin. Journal of Loss Prevention in the Process Industries, 44, 125–131. doi:10.1016/j.jlp.2016.08.024.

[29] Wang, X., Weinell, C. E., Ring, L., & Kiil, S. (2021). Proof of concept investigation of alternative and less harmful boron compounds for epoxy-based hydrocarbon intumescent coatings. Fire Safety Journal, 125, 103437. doi:10.1016/j.firesaf.2021.103437.

[30] Nazrun, T., Hassan, M. K., Hasnat, M. R., Hossain, M. D., Ahmed, B., & Saha, S. (2025). A Comprehensive Review on Intumescent Coatings: Formulation, Manufacturing Methods, Research Development, and Issues. Fire, 8(4), 155. doi:10.3390/fire8040155.

[31] Hu, X., Zhu, X., & Sun, Z. (2019). Efficient flame-retardant and smoke-suppression properties of MgAlCO3-LDHs on the intumescent fire-retardant coating for steel structures. Progress in Organic Coatings, 135, 291–298. doi:10.1016/j.porgcoat.2019.06.014.

[32] Guo, B., Liu, Y., Zhang, Q., Wang, F., Wang, Q., Liu, Y., Li, J., & Yu, H. (2017). Efficient Flame-Retardant and Smoke-Suppression Properties of Mg-Al-Layered Double-Hydroxide Nanostructures on Wood Substrate. ACS Applied Materials and Interfaces, 9(27), 23039–23047. doi:10.1021/acsami.7b06803.

[33] Yorkgitis, E. M., Eiss Jr, N. S., Tran, C., Wilkes, G. L., & McGrath, J. E. (2005). Siloxane-modified epoxy resins. In Epoxy Resins and Composites I, 79-109. doi:10.1007/3-540-15546-5_4.

[34] Chiu, Y. C., Huang, C. C., & Tsai, H. C. (2014). Synthesis, characterization, and thermo mechanical properties of siloxane-modified epoxy-based nano composite. Journal of Applied Polymer Science, 131(21), 40984. doi:10.1002/app.40984.

[35] Lee, Y. X., Ahmad, F., Karuppanan, S., Sumby, C., Shahed, C. A., & Ramli, S. H. (2024). Thermo-mechanical performance of wolframite mineral reinforced siloxane-modified epoxy-based intumescent coating for structural steel. Polymers for Advanced Technologies, 35(1). doi:10.1002/pat.6279.

[36] Hörold, S. (2014). Phosphorus-based and intumescent flame retardants. Polymer Green Flame Retardants, 221-254. doi:10.1016/B978-0-444-53808-6.00006-8.

[37] Wang, G., Huang, Y., & Hu, X. (2013). Synthesis of a novel phosphorus-containing polymer and its application in amino intumescent fire resistant coating. Progress in Organic Coatings, 76(1), 188–193. doi:10.1016/j.porgcoat.2012.09.005.

[38] Chen, L., Song, L., Lv, P., Jie, G., Tai, Q., Xing, W., & Hu, Y. (2011). A new intumescent flame retardant containing phosphorus and nitrogen: Preparation, thermal properties and application to UV curable coating. Progress in Organic Coatings, 70(1), 59–66. doi:10.1016/j.porgcoat.2010.10.002.

[39] Yasir, M., Ahmad, F., Yusoff, P. S. M. M., Ullah, S., & Jimenez, M. (2020). Latest trends for structural steel protection by using intumescent fire protective coatings: a review. Surface Engineering, 36(4), 334–363. doi:10.1080/02670844.2019.1636536.

[40] Anees, S. M., & Dasari, A. (2018). A review on the environmental durability of intumescent coatings for steels. Journal of Materials Science, 53(1), 124–145. doi:10.1007/s10853-017-1500-0.

[41] Lai, Z., Chen, J., Yu, Y., Luo, M., & Li, H. (2024). Effect of magnesium hydroxide on the properties of fireproof coatings for steel structure based on magnesium phosphate cement. Case Studies in Construction Materials, 21. doi:10.1016/j.cscm.2024.e03853.

[42] Fu, A., Ulusoy, B., Ahmadi, H., Wu, H., & Dam-Johansen, K. (2024). Mechanistic study of a silicon-based intumescent coating system. Progress in Organic Coatings, 190, 108354. doi:10.1016/j.porgcoat.2024.108354.

[43] Chen, L., Zeng, S., Xu, Y., Nie, W., Zhou, Y., & Chen, P. (2022). Epoxy-modified silicone resin-based N/P/Si synergistic flame-retardant coating for wood surface. Progress in Organic Coatings, 170, 106953. doi:10.1016/j.porgcoat.2022.106953.

[44] Fu, A., Ahmadi, H., Ulusoy, B., Wu, H., Etxeberria, A. L., & Dam-Johansen, K. (2025). Formulation optimization of a silicon-based fire protective coating in terms of intumescent alkali silicate particles. Construction and Building Materials, 474, 141143. doi:10.1016/j.conbuildmat.2025.141143.

[45] Gillani, Q. F., Ahmad, F., Abdul Mutalib, M. I., Megat-Yusoff, P. S. M., Ullah, S., Messet, P. J., & Zia-ul-Mustafa, M. (2018). Thermal degradation and pyrolysis analysis of zinc borate reinforced intumescent fire-retardant coatings. Progress in Organic Coatings, 123, 82–98. doi:10.1016/j.porgcoat.2018.05.007.

[46] Strassburger, D., Silveira, M. R., Baldissera, A. F., & Ferreira, C. A. (2023). Performance of different water-based resins in the formulation of intumescent coatings for passive fire protection. Journal of Coatings Technology and Research, 20(1), 201–221. doi:10.1007/s11998-021-00597-4.

[47] Zia-ul-Mustafa, M., Ahmad, F., Ullah, S., Amir, N., & Gillani, Q. F. (2017). Thermal and pyrolysis analysis of minerals reinforced intumescent fire-retardant coating. Progress in Organic Coatings, 102, 201–216. doi:10.1016/j.porgcoat.2016.10.014.

[48] Arogundade, A. I., Megat Yussof, P. S. M., Ahmad, F., & Muhammad, I. D. (2025). A Comparative Study of the Reinforcing Effect of Bauxite Residue in Pentaerythritol and Expandable Graphite Based Intumescent Systems. Advanced Materials Research, 1184, 3–12. doi:10.4028/p-ex8ela.

[49] Fan, F. Q., Xia, Z. Bin, Li, Q. Y., & Li, Z. (2013). Effects of inorganic fillers on the shear viscosity and fire-retardant performance of waterborne intumescent coatings. Progress in Organic Coatings, 76(5), 844–851. doi:10.1016/j.porgcoat.2013.02.002.

[50] Wang, X., Song, L., Yang, H., Lu, H., & Hu, Y. (2011). Synergistic effect of graphene on antidripping and fire resistance of intumescent flame-retardant poly(butylene succinate) composites. Industrial and Engineering Chemistry Research, 50(9), 5376–5383. doi:10.1021/ie102566y.

[51] Hsiue, G. H., Liu, Y. L., & Tsiao, J. (2000). Phosphorus-containing epoxy resins for flame retardancy. V: Synergistic effect of phosphorus-silicon on flame retardancy. Journal of Applied Polymer Science, 78(1), 1–7. doi:10.1002/1097-4628(20001003)78:1<1::AID-APP10>3.0.CO;2-0.

[52] Bodzay, B., Bocz, K., Bárkai, Z., & Marosi, G. (2011). Influence of rheological additives on char formation and fire resistance of intumescent coatings. Polymer Degradation and Stability, 96(3), 355–362. doi:10.1016/j.polymdegradstab.2010.03.022.

[53] Chung, Y. C., Kim, J. H., Park, J. E., & Chun, B. C. (2022). Flexible crosslinking of polyurethane using grafted poly(dimethylsiloxane) with Epichlorohydrin and Bisphenol A end groups and its impact on the mechanical properties and low-temperature flexibility. Journal of Elastomers and Plastics, 54(4), 555–573. doi:10.1177/00952443211063599.

[54] Socrates, G. (2004). Infrared and Raman characteristic group frequencies: tables and charts. John Wiley & Sons, New York, United States.

[55] Askar, K. A., & Song, K. (2018). Epoxy-based multifunctional nanocomposites. Polymer-Based Multifunctional Nanocomposites and Their Applications, 2019, 111–135. doi:10.1016/B978-0-12-815067-2.00004-4.

[56] Romo-Uribe, A., Arcos-Casarrubias, J. A., Reyes-Mayer, A., & Guardian-Tapia, R. (2017). PDMS Nanodomains in DGEBA Epoxy Induce High Flexibility and Toughness. Polymer - Plastics Technology and Engineering, 56(1), 96–107. doi:10.1080/03602559.2016.1211691.

[57] Lin, S. T., & Huang, S. K. (1997). Thermal degradation study of siloxane-DGEBA epoxy copolymers. European Polymer Journal, 33(3), 365–373. doi:10.1016/S0014-3057(96)00175-9.

[58] Sobhani, S., Jannesari, A., & Bastani, S. (2012). Effect of molecular weight and content of PDMS on morphology and properties of silicone-modified epoxy resin. Journal of Applied Polymer Science, 123(1), 162–178. doi:10.1002/app.34435.

[59] Sun, X., Chen, R., Gao, X., Liu, Q., Liu, J., Zhang, H., ... & Wang, J. (2019). Fabrication of epoxy modified polysiloxane with enhanced mechanical properties for marine antifouling application. European Polymer Journal, 117, 77-85. doi:10.1016/j.eurpolymj.2019.05.002.

[60] Zhou, C., Li, R., Luo, W., Chen, Y., Zou, H., Liang, M., & Li, Y. (2016). The preparation and properties study of polydimethylsiloxane-based coatings modified by epoxy resin. Journal of Polymer Research, 23(1), 1–10. doi:10.1007/s10965-015-0903-3.

[61] Thanikai Velan, T. V., & Mohammed Bilal, I. (2000). Aliphatic amine cured PDMS-epoxy interpenetrating network system for high performance engineering applications - development and characterization. Bulletin of Materials Science, 23(5), 425–429. doi:10.1007/bf02708394.

[62] Bax, A., Ferretti, J. A., Nashed, N., & Jerina, D. M. (1985). Complete 1H and 13C NMR Assignment of Complex Polycyclic Aromatic Hydrocarbons. Journal of Organic Chemistry, 50(17), 3029–3034. doi:10.1021/jo00217a001.

[63] Hansen, P. E. (1979). 13C NMR of polycyclic aromatic compounds. A review. Organic Magnetic Resonance, 12(3), 109–142. doi:10.1002/mrc.1270120302.

[64] Miyajima, G., & Nishimoto, K. (1974). Carbon-13 nuclear magnetic resonance spectroscopy: VIII—aliphatic hydrocarbon derivatives. Organic Magnetic Resonance, 6(6), 313–321. doi:10.1002/mrc.1270060604.

[65] Sima, W., Pang, W., Sun, P., Yuan, T., Yang, M., Chen, X., Li, Z., Liu, X., & Tang, X. (2024). Design of epoxy composites via molecular orbital modulation and enhanced π-πF interactions achieving synchronous improvement of electrical and mechanical performance. Chemical Engineering Journal, 500, 156745. doi:10.1016/j.cej.2024.156745.

[66] Cook, M., & Harper, J. F. (1998). The influence of magnesium hydroxide morphology on the crystallinity and properties of filled polypropylene. Advances in Polymer Technology, 17(1), 53–62. doi:10.1002/(SICI)1098-2329(199821)17:1<53::AID-ADV5>3.0.CO;2-H.

[67] Lan, S., Zhu, D., Li, L., Liu, Z., Zeng, Z., & Song, F. (2018). Surface modification of magnesium hydroxide particles using silane coupling agent by dry process. Surface and Interface Analysis, 50(3), 277–283. doi:10.1002/sia.6363.

[68] Dreyfuss, P. (1978). Chemistry of Silane Coupling Reactions. 1. Reaction of Trimethylmethoxysilane and Triethylsilanol Studied by Gas-Liquid Chromatography. Macromolecules, 11(5), 1031–1036. doi:10.1021/ma60065a035.

[69] Thirumalaikumar, M. (2022). Ring Opening Reactions of Epoxides. A Review. Organic Preparations and Procedures International, 54(1), 1–39. doi:10.1080/00304948.2021.1979357.

[70] Branda, F., Passaro, J., Pauer, R., Gaan, S., & Bifulco, A. (2022). Solvent-Free One-Pot Synthesis of Epoxy Nanocomposites Containing $Mg(OH)_2$ Nanocrystal−Nanoparticle Formation Mechanism. Langmuir, 38(18), 5795–5802. doi:10.1021/acs.langmuir.2c00377.

[71] Díaz, U., Brunel, D., & Corma, A. (2013). Catalysis using multifunctional organosiliceous hybrid materials. Chemical Society Reviews, 42(9), 4083–4097. doi:10.1039/c2cs35385g.

[72] Wang, Y., Yan, L., Ling, Y., Ge, Y., Huang, C., Zhou, S., Xia, S., Liang, M., & Zou, H. (2023). Enhanced mechanical and adhesive properties of PDMS coatings via in-situ formation of uniformly dispersed epoxy reinforcing phase. Progress in Organic Coatings, 174(107319). doi:10.1016/j.porgcoat.2022.107319.

[73] Wang, Y., Cai, Y., Ling, Y., Zhang, H., Tian, J., Heng, Z., Zhou, S., Xia, S., Liang, M., & Zou, H. (2023). Improved Mechanical and Ablative Properties of PDMS Coatings Incorporating Epoxy as a Suspended Chain. Industrial and Engineering Chemistry Research, 62(25), 9920–9931. doi:10.1021/acs.iecr.3c00814.

[74] Zope, I. S. (2018). Fire retardancy behavior of polymer/clay nanocomposites. Springer, Berlin, Germany. doi:10.1007/978-981-10-8327-3.

[75] Yang, Y., Niu, M., Bai, J., Xue, B., & Dai, J. (2018). Preparation of microencapsulated carbon microspheres coated by magnesium hydroxide/polyethylene terephthalate flame–retardant functional fibers and its flame-retardant properties. Journal of the Textile Institute, 109(4), 445–454. doi:10.1080/00405000.2017.1351655.

[76] Wilkie, C. A., & Morgan, A. B. (2024). Fire retardancy of polymeric materials. CRC Press, Florida, United States. doi:10.1201/9781003380689.

[77] Jimenez, M., Duquesne, S., & Bourbigot, S. (2006). Intumescent fire protective coating: Toward a better understanding of their mechanism of action. Thermochimica Acta, 449(1–2), 16–26. doi:10.1016/j.tca.2006.07.008.

[78] Guo, F., Zhang, Y., Cai, L., & Li, L. (2022). Functionalized graphene with Platelet-like magnesium hydroxide for enhancing fire safety, smoke suppression and toxicity reduction of Epoxy resin. Applied Surface Science, 578, 152052. doi:10.1016/j.apsusc.2021.152052.

[79] Qiu, X., Li, Z., Li, X., & Zhang, Z. (2018). Flame retardant coatings prepared using layer by layer assembly: A review. Chemical Engineering Journal, 334, 108–122. doi:10.1016/j.cej.2017.09.194.

[80] Laoutid, F., Bonnaud, L., Alexandre, M., Lopez-Cuesta, J. M., & Dubois, P. (2009). New prospects in flame retardant polymer materials: From fundamentals to nanocomposites. Materials Science and Engineering R: Reports, 63(3), 100–125. doi:10.1016/j.mser.2008.09.002.

[81] Yang, J., Chen, X., Zhou, H., Guo, W., Zhang, J., Miao, Z., & He, D. (2022). Synergistic effect of expandable graphite and aluminum hypophosphite in flame-retardant ethylene vinyl acetate composites. Polymers for Advanced Technologies, 33(2), 638–646. doi:10.1002/pat.5546.

[82] Zhang, H., Zhang, D. Z., Wang, D. Y., Xu, Z. Y., Yang, Y., & Zhang, B. (2022). Flexible single-electrode triboelectric nanogenerator with MWCNT/PDMS composite film for environmental energy harvesting and human motion monitoring. Rare Metals, 41(9), 3117–3128. doi:10.1007/s12598-022-02031-z.

[83] Wang, Y., Cai, Y., Zhang, H., Zhou, J., Zhou, S., Chen, Y., Liang, M., & Zou, H. (2021). Mechanical and thermal degradation behavior of high-performance PDMS elastomer based on epoxy/silicone hybrid network. Polymer, 236, 124299. doi:10.1016/j.polymer.2021.124299.

[84] Azmi, Y., Ahmad, F., Kabir, S., Lee, Y. X., Zulfiqar, A., Yeoh, G. H., Qaiser, A., & Masset, P. J. (2023). Investigating the Mechanical Performance of Intumescent Coating Enhanced with Magnesium Oxide (MgO) for Structural Steel Application. Lecture Notes in Mechanical Engineering, 927–938. doi:10.1007/978-981-19-1939-8_69.

[85] Wang, F., Liu, H., & Yan, L. (2021). Comparative study of fire resistance and char formation of intumescent fire-retardant coatings reinforced with three types of shell bio-fillers. Polymers, 13(24), 4333. doi:10.3390/polym13244333.

[86] Mróz, K., Hager, I., & Korniejenko, K. (2016). Material Solutions for Passive Fire Protection of Buildings and Structures and Their Performances Testing. Procedia Engineering, 151, 284–291. doi:10.1016/j.proeng.2016.07.388.

[87] Ahmed, H. B., Ramadan, A. M., Nour, M. A., Abd el-Malak, S. S., & Gomaa, A. E. A. Z. (2018). Innovative precursor for manufacturing of superior enhancer of intumescence for paint: Thermal insulative coating for steel structures. Progress in Organic Coatings, 118, 129–140. doi:10.1016/j.porgcoat.2018.01.017.

[88] Wang, S., Wang, X., Wang, X., Li, H., Sun, J., Sun, W., Yao, Y., Gu, X., & Zhang, S. (2020). Surface coated rigid polyurethane foam with durable flame retardancy and improved mechanical property. Chemical Engineering Journal, 385, 123755. doi:10.1016/j.cej.2019.123755.

[89] Jefferson Andrew, J., Sain, M., Ramakrishna, S., Jawaid, M., & Dhakal, H. N. (2024). Environmentally friendly fire-retardant natural fibre composites: A review. International Materials Reviews, 69(5–6), 267–308. doi:10.1177/09506608241266302.

[90] Yeoh, G. H., De Cachinho Cordeiro, I. M., Wang, W., Wang, C., Yuen, A. C. Y., Chen, T. B. Y., ... & Chua, H. T. (2024). Carbon‐based flame retardants for polymers: a bottom‐up review. Advanced Materials, 36(42), 2403835. doi:10.1002/adma.202403835.

[91] Wang, Z., Han, E., & Ke, W. (2006). Effect of nanoparticles on the improvement in fire-resistant and anti-ageing properties of flame-retardant coating. Surface and Coatings Technology, 200(20–21), 5706–5716. doi:10.1016/j.surfcoat.2005.08.102.

[92] Reich, S. J., Svidrytski, A., Höltzel, A., Wang, W., Kübel, C., Hlushkou, D., & Tallarek, U. (2019). Transport under confinement: Hindrance factors for diffusion in core-shell and fully porous particles with different mesopore space morphologies. Microporous and Mesoporous Materials, 282, 188–196. doi:10.1016/j.micromeso.2019.02.036.

[93] Bo, L., Hua, G., Xian, J., Zeinali Heris, S., Erfani Farsi Eidgah, E., Ghafurian, M. M., & Orooji, Y. (2024). Recent remediation strategies for flame retardancy via nanoparticles. Chemosphere, 354, 141323. doi:10.1016/j.chemosphere.2024.141323.

[94] Camino, G., Costa, L., & Trossarelli, L. (1984). Mechanism of Intumescence in Fire Retardant Additives for Polymers. American Chemical Society, Polymer Preprints, Division of Polymer Chemistry, 25(1), 90.

[95] Horrocks, A. R., & Price, D. (Eds.). (2008). Advances in fire retardant materials. Elsevier, Amsterdam, Netherlands. doi:10.1533/9781845694701.

[96] Zybina, O., & Gravit, M. (2020). Intumescent coatings for fire protection of building structures and materials. Springer, Cham, Switzerland. doi:10.1007/978-3-030-59422-0.

[97] Dorn, P. B., Chou, C. S., & Gentempo, J. J. (1987). Degradation of bisphenol A in natural waters. Chemosphere, 16(7), 1501–1507. doi:10.1016/0045-6535(87)90090-7.

[98] Levchik, S. V., & Weil, E. D. (2004). Thermal decomposition, combustion and flame-retardancy of epoxy resins - A review of the recent literature. Polymer International, 53(12), 1901–1929. doi:10.1002/pi.1473.

[99] Wang, H., Wang, Q., Huang, Z., & Shi, W. (2007). Synthesis and thermal degradation behaviors of hyperbranched polyphosphate. Polymer Degradation and Stability, 92(10), 1788–1794. doi:10.1016/j.polymdegradstab.2007.07.008.

[100] Li, J., Wang, H., & Li, S. (2019). A novel phosphorus−silicon containing epoxy resin with enhanced thermal stability, flame retardancy and mechanical properties. Polymer Degradation and Stability, 164, 36–45. doi:10.1016/j.polymdegradstab.2019.03.020.

[101] Jia, P., Liu, H., Liu, Q., & Cai, X. (2016). Thermal degradation mechanism and flame retardancy of MQ silicone/ epoxy resin composites. Polymer Degradation and Stability, 134, 144–150. doi:10.1016/j.polymdegradstab.2016.09.029.

[102] Niemczyk, A., Dziubek, K., Sacher-Majewska, B., Czaja, K., Czech-Polak, J., Oliwa, R., Lenza, J., & Szołyga, M. (2018). Thermal stability and flame retardancy of polypropylene composites containing siloxane-silsesquioxane resins. Polymers, 10(9), 1019. doi:10.3390/polym10091019.

[103] Jimenez, M., Duquesne, S., & Bourbigot, S. (2012). Fire protection of polypropylene and polycarbonate by intumescent coatings. Polymers for Advanced Technologies, 23(1), 130–135. doi:10.1002/pat.1809.

[104] Thabah, S., Rai, A. K., & Joshi, S. R. (2025). Geomicrobes in Environmental Remediation of Polyaromatic Hydrocarbons. Mineral Transformation and Bioremediation by Geo-Microbes. Springer, 2025, 415–431. doi:10.1007/978-981-96-3033-2_16.

[105] Wang, Q. (2015). Preparation and surface modification of Mg(OH)2/siloxane nanocomposite flame retardant. Journal of Polymer Engineering, 35(2), 113–117. doi:10.1515/polyeng-2014-0032.

[106] Ning, Y., & Guo, S. (2000). Flame-retardant and smoke-suppressant properties of zinc borate and aluminum trihydrate-filled rigid PVC. Journal of Applied Polymer Science, 77(14), 3119–3127. doi:10.1002/1097-4628(20000929)77:14<3142::AID-APP150>3.0.CO;2-2.

[107] Hameed, N. A., Abbas, S. J., Thamer, M. J., & Abbas, S. Q. (2022). Implementation of the Mgo/Epoxy Nanocomposites as Flame Retardant. Eastern-European Journal of Enterprise Technologies, 3(6–117), 53–57. doi:10.15587/1729-4061.2022.260359.

[108] Gillani, Q. F., Ahmad, F., Melor, P. S., Mutlib, M. I. A., & Ullah, S. (2018). A synergy study of zinc borate in halloysite nanotube reinforced, siloxane epoxy base intumescent fire resistive coatings: Eine Synergieuntersuchung zu Zinkborat in, mit Halloysit-Nanoröhren verstärkten, Siloxane Epoxy basierten, intumeszenten feuerfesten Beschichtungen. Materialwissenschaft Und Werkstofftechnik, 49(4), 420–426. doi:10.1002/mawe.201700254.

[109] Murat Unlu, S., Tayfun, U., Yildirim, B., & Dogan, M. (2017). Effect of boron compounds on fire protection properties of epoxy based intumescent coating. Fire and Materials, 41(1), 17–28. doi:10.1002/fam.2360.

[110] Otáhal, R., Veselý, D., Násadová, J., Zíma, V., Němec, P., & Kalenda, P. (2011). Intumescent coatings based on an organic-inorganic hybrid resin and the effect of mineral fibres on fire-resistant properties of intumescent coatings. Pigment and Resin Technology, 40(4), 247–253. doi:10.1108/03699421111147326.

[111] Nandiyanto, A. B. D., Oktiani, R., & Ragadhita, R. (2019). How to read and interpret ftir spectroscope of organic material. Indonesian Journal of Science and Technology, 4(1), 97–118. doi:10.17509/ijost.v4i1.15806.

[112] Wang, L. L., Wang, Y. C., & Li, G. Q. (2013). Experimental study of hydrothermal aging effects on insulative properties of intumescent coating for steel elements. Fire Safety Journal, 55, 168–181. doi:10.1016/j.firesaf.2012.10.004.

[113] Balakrishnan, G., Velavan, R., Mujasam Batoo, K., & Raslan, E. H. (2020). Microstructure, optical and photocatalytic properties of MgO nanoparticles. Results in Physics, 16, 103013. doi:10.1016/j.rinp.2020.103013.

[114] Stec, A. A. (2017). Fire toxicity–the elephant in the room?. Fire Safety Journal, 91, 79-90. doi:10.1016/j.firesaf.2017.05.003.

[115] Babrauskas, V. (2008). Quantifying the combustion product hazard on the basis of test results. Hazards of combustion products: toxicity, opacity, corrosivity and heat release. London: Interscience Communications, 339-353.

[116] Verma, N., Pink, M., Rettenmeier, A. W., & Schmitz-Spanke, S. (2012). Review on proteomic analyses of benzo[a]pyrene toxicity. Proteomics, 12(11), 1731–1755. doi:10.1002/pmic.201100466.

[117] English, C. (2022). Understanding the origins of siloxane ghost peaks in gas chromatography. Column (LCGC International), 18, 10-15.

[118] Puri, R. G., & Khanna, A. S. (2017). Intumescent coatings: A review on recent progress. Journal of Coatings Technology and Research, 14(1), 1-20. doi:10.1007/s11998-016-9815-3.

[119] de Sá, S. C., de Souza, M. M., Peres, R. S., Zmozinski, A. V., Braga, R. M., de Araújo Melo, D. M., & Ferreira, C. A. (2017). Environmentally friendly intumescent coatings formulated with vegetable compounds. Progress in Organic Coatings, 113, 47–59. doi:10.1016/j.porgcoat.2017.08.007.

Appendix I

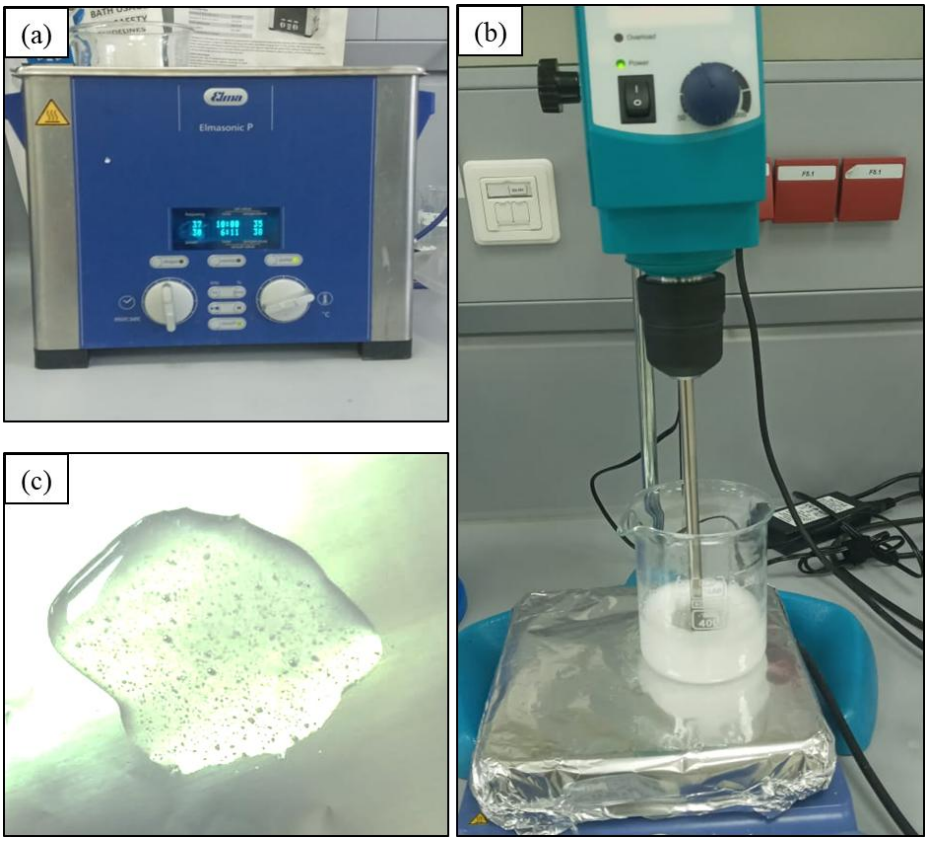

Figure A-1. Dispersion process of magnesium hydroxide ($Mg(OH)_2$) in bisphenol-A epoxy resin:(a) Ultrasonic bath (Elma Elmasonic P) used for high-energy sonication of $Mg(OH)_2$ particles;(b) High-shear mechanical mixer setup used for initial dispersion at 3500 rpm for 20 minutes;(c) Visual appearance of the epoxy-$Mg(OH)_2$ dispersion showing good distribution after processing.

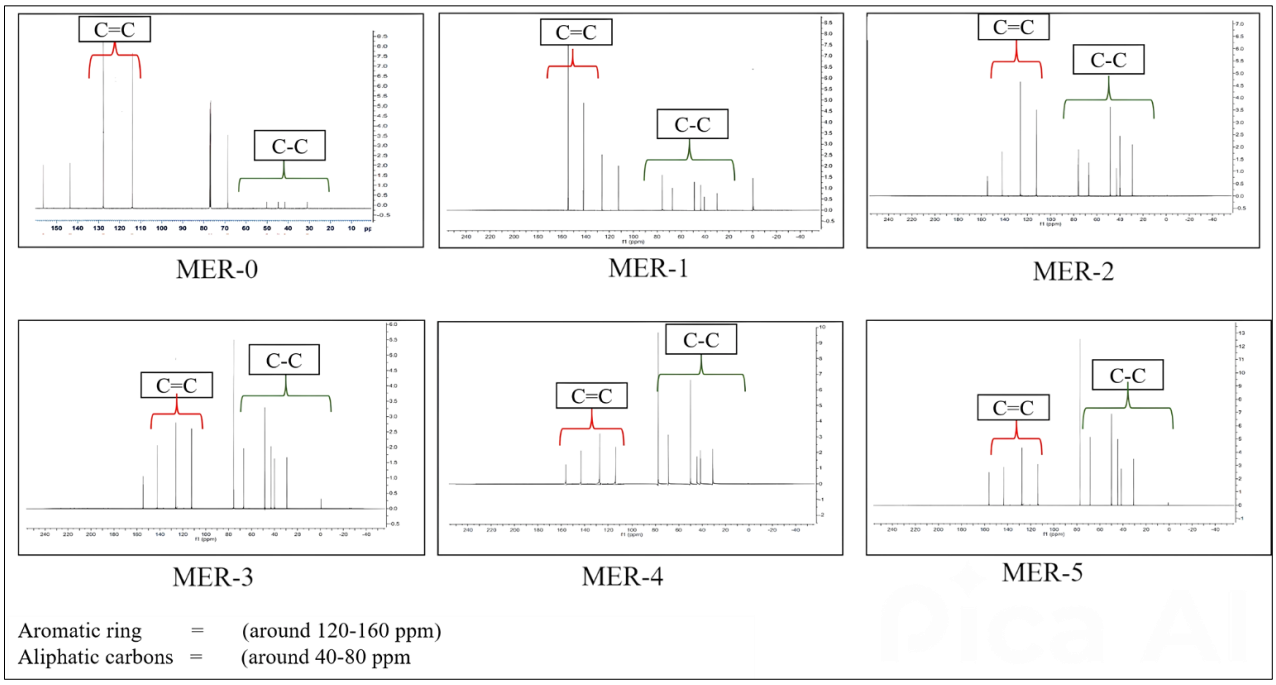

Figure A-2. Structural evolution of epoxy resins observed through ^{13}C NMR spectroscopy

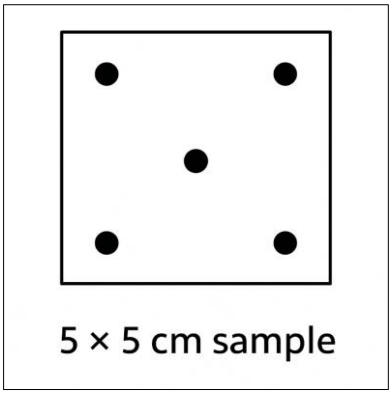

Figure A-3. Schematic of a 5 × 5 cm coated steel sample showing the five measurement points (one center, four corners) used for expansion thickness determination. All points are positioned at equal distances **from each other to ensure consistent averaging.**

Figure A-4. IF-3 coated samples before and after fire test